International Journal of Refrigeration 86 (2018) 239–257

Contents lists available at ScienceDirect

International Journal of Refrigeration

journal homepage: www.elsevier.com/locate/ijrefrig

State-of-the-art integrated CO_2 refrigeration system for supermarkets: A comparative analysis

Mazyar Karampour*, Samer Sawalha

Royal Institute of Technology (KTH), Energy Technology Department, Brinellvägen 68, SE-100 44 Stockholm, Sweden

ARTICLE INFO

Article history:
Received 1 August 2017
Revised 2 November 2017
Accepted 3 November 2017
Available online 10 November 2017

Keywords:
CO_2 trans-critical booster system
Supermarket
State-of-the-art
System integration

ABSTRACT

This paper investigates the integrated and state-of-the art features of CO_2 trans-critical booster systems. The main objective is to identify the most promising solutions in terms of energy efficiency impacts.

First, the performance of modified features and integrated functions have been compared with the standard CO_2 system and alternative heating and air conditioning solutions. Subsequently, the performance of the defined state-of-the-art CO_2 system is compared to natural refrigerant-based cascade and HFC/HFO-based DX and indirect refrigeration solutions operating in cold and warm climates.

The results indicate that two-stage heat recovery, flooded evaporation, parallel compression and integration of air conditioning are the most promising features of the state-of-the-art integrated CO_2 system. This compact and environmentally friendly system is the most energy efficient solution in cold climates, and is also an efficient solution in warm climates, with comparable efficiency to cascade and HFC/HFO DX systems, but with no existing or potential limitations.

1. Introduction

The CO_2 trans-critical booster system has become the standard supermarket refrigeration solution for new installations in some European countries, mainly the Scandinavian countries. This technology acceptance originated from the fact that the system outperforms the conventional synthetic refrigerant-based system in cold climates (Finckh et al., 2011; Sawalha et al., 2017; Karampour and Sawalha, 2017). The heat recovery from this system is an appealing choice to provide the heating demands of supermarket (Reinholdt and Madsen, 2010; Sawalha, 2013). Furthermore, it avoids the ever-lasting concerns of following environmental regulations and restrictions. The installation and operating cost of the system has become comparable to conventional solutions (Zeiger et al., 2016).

There are two main innovation approaches pushing and spreading the applications of this system further south of Europe and beyond. The first is integration of all thermal functions in one compact unit. Air conditioning and heating integration provides a compact "plug & play" energy system, using electricity as the source energy and CO_2 as an environmentally friendly refrigerant. Compared to a complete stand-alone system, the integrated solution requires fewer components and less refrigerant. This contributes to a considerable space saving. Furthermore, in larger supermarkets the integrated functions are provided by a set of compressors. This reduces the risk of service interruption in case of one compressor failure (compared to stand-alone systems). Finally, the integration provides better control communications between the HVAC&R systems.

The second approach is to modify the "standard CO_2 system" to increase its energy efficiency, focusing on warm climate operation. Flooded evaporation by ejectors, parallel compression, mechanical sub-cooling and gas cooler evaporative cooling are some of the most recently applied modifications introduced into the supermarket refrigeration sector. Some modification options including mechanical sub-cooling and evaporative cooling improve the gas cooling process and provide higher energy efficiency in warm climates, while features such as flooded evaporation improves the system energy efficiency in any climate.

The energy efficiency impacts of these modified features and integrated functions are presented and discussed by various researchers. The following are samples of the researches which investigate the positive impacts of single modifications; single or multi-ejectors (Hafner et al., 2014; Gullo et al., 2017; Schönenberger et al., 2014), parallel compression (Javerschek et al., 2015; Javerschek et al., 2016; Karampour and Sawalha, 2015), flooded evaporation (Minetto et al., 2014a; Tambovtsev and Quack, 2007), mechanical sub-cooling (Llopis et al., 2016a; Bush et al., 2017), evaporative cooling (Girotto and Minetto, 2008; Lozza et al., 2007), and LT de-superheater (Llopis et al., 2016b).

* Corresponding author.
E-mail addresses: mazyar.karampour@energy.kth.se (M. Karampour), samer.sawalha@energy.kth.se (S. Sawalha).

https://doi.org/10.1016/j.ijrefrig.2017.11.006
0140-7007/

Nomenclature

AC	air conditioning
ASHP	air source heat pump
COP	coefficient of performance
DX	direct expansion
GSHP	ground source heat pump
GWP	Global Warming Potential
HFC	hydrofluorocarbon
HP	heat pump
HR	heat recovery
LR	load ratio
LT	low temperature level
MT	medium temperature level
PC	parallel compression
Ref	refrigeration/refrigerant
SotA	state-of-the-art
TEWI	Total Equivalent Warming Impact
€/k€	euros/thousand euros

Variables

AEU	annual energy use, MWh
f	frequency, number of hours
$\dot{E}$	electric power, kW
h	enthalpy per unit mass, kJ kg^{-1}
M	mass, kg
$\dot{m}$	mass flow rate, kg s^{-1}
N	lifetime, years
n	number of temperature-bins
P	pressure, bar
$\dot{Q}$	cooling or heating load, kW
RC	electricity regional conversion factor, kgCO_2 kWh^{-1}
T	temperature, °C
SPF	seasonal performance factor
SEER	seasonal energy efficiency ratio
Δ	difference
κ	recycle factor
η	efficiency of compressor

Subscripts

AC	air conditioning
amb	ambient
comp	compressor
el	electricity
fan	gas cooler/condenser fans
gc	gas cooler
HR	heat recovery
is	isentropic
LT	low temperature level
MT	medium temperature level
opt	optimal
PC	parallel compression
ref	refrigeration/refrigerant
max	maximum
return	hot water return
SPH	Space heating
supply	hot water supply
tot	total
TWH	tap water heating

The research on systems integration is reviewed comprehensively by Karampour and Sawalha (2017). To mention some of these research works, heat recovery is studied by Sawalha (2013), Reinholdt and Madsen (2010), Polzot et al. (2017), Nöding et al. (2016) and the integration of air conditioning is discussed by Hafner et al. (2016), Karampour and Sawalha (2016a), Girotto (2016) and Gullo et al. (2017).

There is a risk that this variety of choices creates confusion. A shortcoming in the research and literature is to have a holistic approach examining all the alternative cooling and heating solutions to ease the decision- making process for supermarket stake holders on what to implement as the essential and most promising energy efficiency measures in the supermarket thermal energy systems.

What distinguishes this paper from previous research is that all the established energy efficiency features and concepts are studied in order to define the state-of-the-art integrated CO_2 system. Subsequently, this system performance is compared to modern alternative refrigeration, heating and air conditioning systems. The comparison assumptions are based on updated improvements in the components, control strategies and safety of all the systems.

The objective of this paper is to study and define the state-of-the-art integrated CO_2 trans-critical booster refrigeration system. To fulfil this objective, three approaches are adapted:

First, the energy efficiency impacts of modified features are studied. Second, the performance of functions integrated into the CO_2 system is compared to alternative stand-alone heating and air conditioning systems. The state-of-the-art integrated CO_2 system is defined based on the results of these two steps. Finally, energy performance and environmental aspects of the defined state-of-the-art CO_2 system are compared to alternative advanced and modern refrigeration system solutions including HFC/HFO DX and indirect systems, and cascade ammonia–CO_2 and propane–CO_2 systems.

The structure of the papers is as follows: standard and state-of-the-art CO_2 systems and their alternative refrigeration solutions are described in Section 2. The modelling details including assumptions and calculation methods are described in Section 3. The first part of the research results is presented in Section 4.1; it includes the evaluation of the standard CO_2 system modified features in order to define the "state-of-the-art" CO_2 system. The second part of the results, presented in Section 4.2, discusses the comparisons between the state-of-the-art CO_2 system and the alternative refrigeration solutions.

2. System description

2.1. CO_2 standard and state-of-the-art systems

The schematic of a standard CO_2 trans-critical booster system and its sample P-h diagram is shown in Fig. 1-left. The system has become a well-established solution over the past 5–10 years, and its operation has been described in various publications such as Sawalha et al. (2015), Finckh and Sienel (2010), Javerschek (2008), Ommen and Elmegaard (2012) and Matthiesen et al. (2010). Some features are considered standard in this system due to their proven positive impact on efficiency. Such features are: flash gas by-pass, heat recovery (HR), high pressure optimisation control, glass doors-lids on freezers and cabinets, and one variable speed compressor in each compression unit.

This standard solution has been subject to continuous modification to increase its energy efficiency. In this paper, the most promising modifications are studied in order to identify the key features of a state-of-the-art system.

A schematic of a state-of-the-art system (SotA) with its key features and its sample P-h diagram is shown in Fig. 1-right. The most important measurements including compressor electric powers and pressures are shown in this figure. The loads are also shown including medium temperature refrigeration $\dot{Q}_{MT}$, low temperature refrigeration $\dot{Q}_{LT}$, air conditioning $\dot{Q}_{AC}$, tap water heating $\dot{Q}_{TWH}$, and space heating $\dot{Q}_{SPH}$. The latter three integrated loads are shown schematically in the P-h diagram.

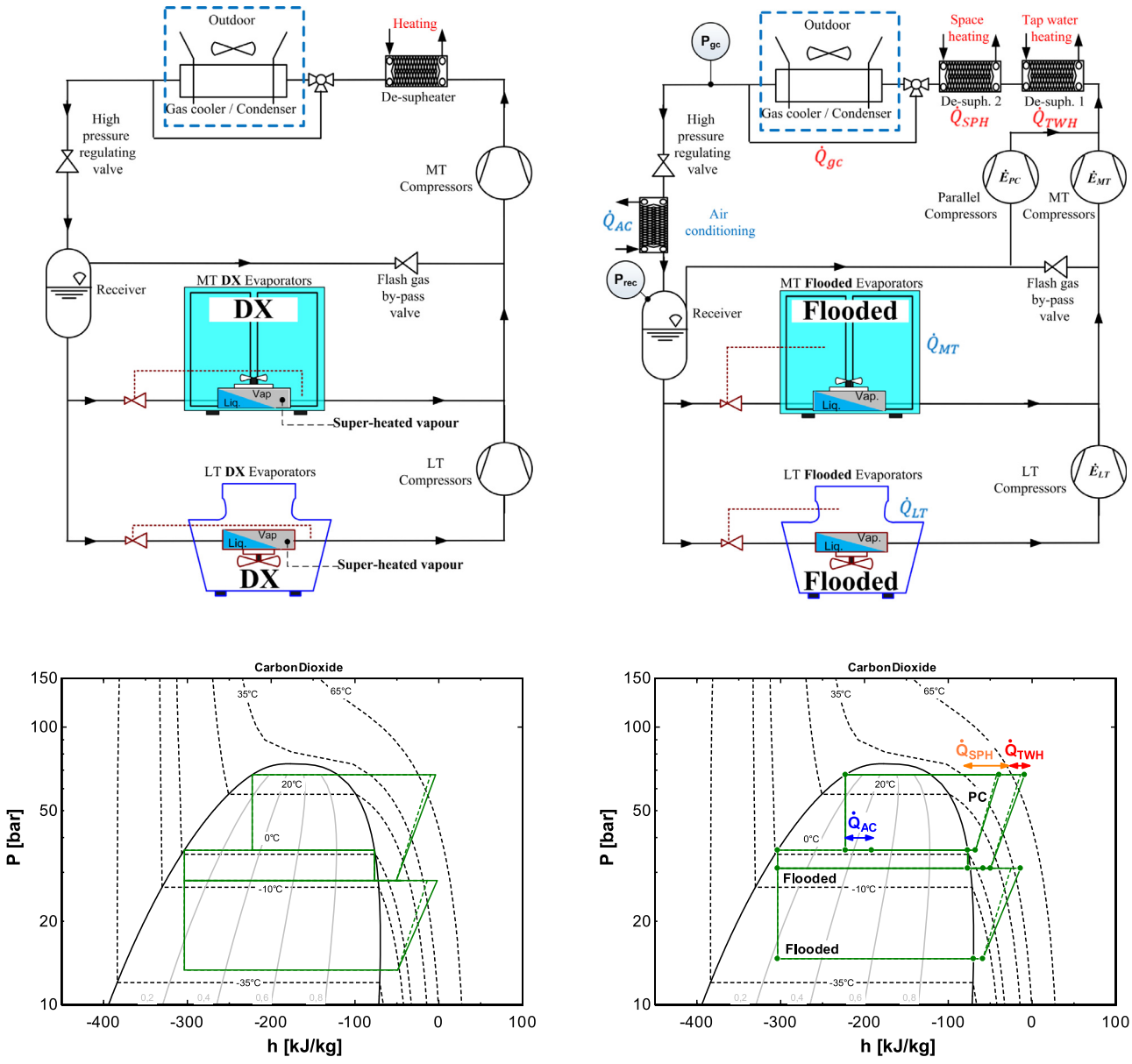

Fig. 1. Schematic and *P–h* diagrams of a standard CO_2 booster system (left) a state-of-the-art CO_2 booster system (right).

One of the major differences from the standard system is on running the MT and LT evaporators in flooded evaporation condition. The evaporators are run in DX condition in the CO_2 standard system. It means a section of the evaporator is specified for superheating of the refrigerant. It is widely known that the heat transfer coefficient in the two phase flow region is significantly higher than this single phase super-heater section of the evaporator. On the contrary, the flooded evaporator takes the advantage of liquid CO_2 evaporation down to the exit of the evaporator. This higher heat transfer coefficient and no super-heating results in higher evaporation temperatures compared to the conventional DX systems. Methods for how to implement flooded evaporation are discussed in Section 4.1.2. Another difference is on processing the vapour out from the receiver, where parallel compression (PC) is used to compress this vapour at higher suction pressures compared to the case in the standard system. Heat recovery in the state-of-the-art system is provided in two stages (i.e. heat exchangers in series) for tap water and space heating. Two-stage heat recovery might provide a better separated control for the desired demands and also helps avoid the pinch point occurrence inside the de-superheater, which is more probable in one-stage heat recovery.

Integration of air conditioning (AC) into the CO_2 booster system is a compact solution. This can be done by adding a heat exchanger between the high pressure regulating valve and the receiver. An alternative AC heat exchanger arrangement is a thermosiphon loop fed from the liquid part of the receiver. AC delivery should be accompanied by running parallel compressors.

The impacts of the mentioned features on system energy efficiency are evaluated in Section 4.1. The refrigeration performance of standard and state-of-the-art CO_2 systems are compared to some alternative refrigeration solutions in Section 4.2.

2.2. Direct expansion (DX) and indirect HFC/HFO solutions

The most conventional supermarket refrigeration solution in Europe is an R404A DX with separate MT and LT refrigeration units. This refrigeration system represents the present conventional system on the European market. However, this solution is being

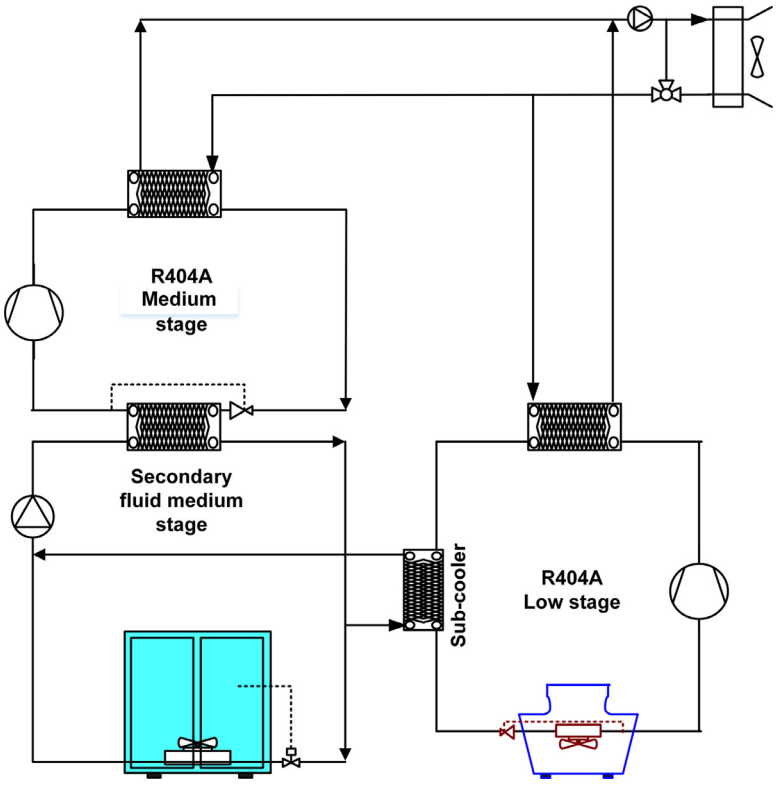

Fig. 2. Basic schematic diagram of an R404A indirect system.

phased out due to its high GWP (GWP = 3922). The suggested drop-ins for R404A are mixtures of HFC and HFO (non-saturated HFC) refrigerants or just mixture of HFCs. R448A (GWP = 1387), R449A (GWP = 1397) and R407H (GWP = 1495) are some of these HFC or HFC/HFO mixtures which may replace R404A in some supermarkets in Europe. There are few research discussing this replacement comprehensively (Makhnatch et al., 2017). In this study, R449A is selected to represent this new generation of synthetic refrigerants.

The conventional refrigeration system in Sweden has been an indirect R404A system as presented comprehensively by Sawalha et al. (2017) and shown in Fig. 2. This refrigeration system is composed of two R404A loops; LT loop in the freezers is a DX R404A unit, while the MT loop consists of an indirect secondary fluid cycle (for example, propylene glycol or ethylene glycol) connecting the MT cabinets to an R404A refrigeration unit. The refrigerant exiting the LT condenser is sub-cooled by the MT secondary fluid. On the high-pressure side, the heat from MT and LT condensers are rejected to the ambient by indirect secondary fluid cycles connected to a dry cooler. The reason for implementing these indirect loops is to limit the refrigerant charge of R404A. The assumptions of HFC/HFO systems modelling are summarised in Table 2.

2.3. Cascade ammonia–CO_2 and propane–CO_2 solutions

An alternative solution to the CO_2 booster system is a cascade system. The natural refrigerants ammonia (GWP = 0) and propane (GWP = 3), which were used in the early stage of cascade CO_2 refrigeration development, were considered hazardous and their development did not become more widespread. However, more compact and safer ammonia and propane systems and components are developed nowadays, and the required charge is reduced significantly (Shecco, 2016, 2015). According to the F-gas regulations, HFCs and HFOs with GWP lower than 1500 are also allowed to be used in the high stage of cascade solutions (EU 517/2014, 2014) and some other research presented these systems (Llopis et al., 2016b; Gullo and Cortella, 2016; Beshr et al., 2015). However, it is intended to present fully natural refrigerant-based cascade systems in this paper, as an alternative climate friendly and future proof solution.

A cascade system configuration is shown in Fig. 3. The cascade system is composed of CO_2 in the LT and MT refrigeration loops and ammonia or propane on the high stage. To confine the charge of high stage refrigerant and minimise the leakage risks, the heat from the high stage is rejected to the ambient through an indirect secondary fluid loop. CO_2 in the LT stage is flooded using internal heat exchanger (IHX) and is flooded with pump circulation in the MT loop. The flooded evaporation is discussed in detail in Section 4.1.2. On the high stage, an IHX is used so as to provide sub-cooling at the exit of the condenser and super-heating at the compressor inlet. The main assumptions and discussions of these systems modelling are presented in Section 4.2 and summarised in Table 2.

3. Modelling details

To define the input to the computer modellings, Stockholm, Sweden is used as the reference case. Barcelona, Spain, is selected as a city representing warm climate regions. Unless otherwise stated, the same inputs as for Stockholm are applied to Barcelona.

3.1. Boundary conditions and assumptions

To preserve the quality of chilled and frozen food products, air temperature is typically kept below + 3 °C and −18 °C in the cabinets and freezers. CO_2 evaporation temperatures in MT and LT levels are assumed to be −8 °C and −32 °C in the standard system. Internal and external super-heatings are assumed to be both 10 K at MT and LT levels. These assumptions are based on field measurement observations of five Swedish supermarkets using CO_2 as the

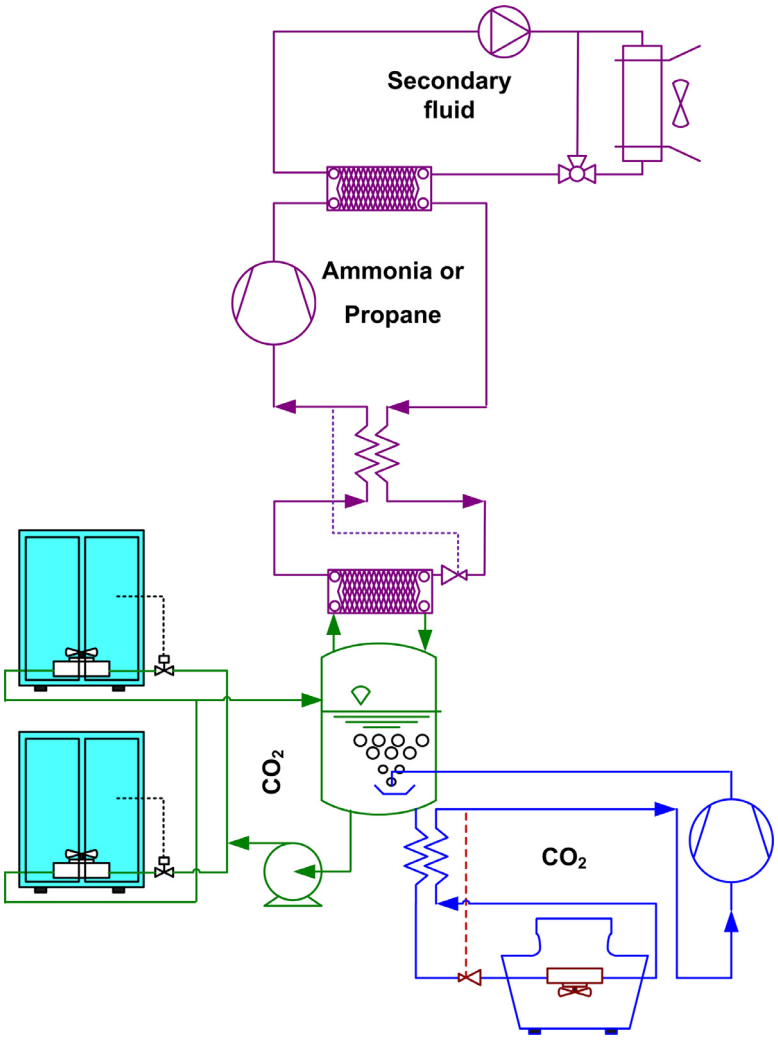

Fig. 3. Schematic of an ammonia–CO_2 or a propane–CO_2 cascade system.

refrigerant (Sawalha et al., 2015). The evaporators in the state-of-the-art system are flooded, which results in 3–4 K higher evaporation temperatures and it is assumed that the internal super-heating is zero in this case, i.e. the exit vapour is in saturated condition. More details on this assumption are explained in Section 4.1.2.

The refrigeration and heating demands are obtained by the program CyberMart for a medium-sized supermarket in Sweden, and the calculated loads are checked to have similar trends to those observed in the field measurement analysis. CyberMart is a tool to investigate and compare the annual energy use of different refrigeration systems in supermarkets. The software estimates the refrigeration capacities and the corresponding electricity use based on the selected display cabinets and indoor climate conditions. The indoor climate conditions is calculated using interactions between the outdoor climate, building envelope, indoor heat gains and installed HVAC solutions. Detailed descriptions and calculations of the program can be found in the Doctoral Thesis by Arias (2005).

The cooling demand at MT level is dependent on the ambient temperature. It is assumed to be 200 kW at 35 °C, and decreases linearly to 100 kW at 10 °C. For ambient temperatures lower than 10 °C, the MT cooling demand is assumed to remain constant at 100 kW. The main reason that cooling demand follows the ambient temperature is the lack of glass doors in the cabinets. The humidity content of the ambient air increases during summer, and this results in an increase in the indoor humidity. The low temperature level freezers are typically covered by glass lids, and field measurement analysis has shown that it remains almost constant with minor fluctuations through the entire year (Sawalha et al., 2015; 2017; Karampour and Sawalha, 2017). 35 kW of LT cooling demand is assumed for the entire year in the simulation.

The main heating demand in supermarkets is space heating, and the set point to start supplying the heat is 10 °C ambient temperature. Based on CyberMart's calculations, it is estimated that at 10 °C the heating demand is 40 kW for a medium-sized Swedish supermarket, and it increases linearly to 190 kW at −20 °C ambient temperature.

Heat is recovered in the space heating de-superheater with the water return temperature as a function of ambient temperature. The space heating system's forward and return water temperatures are assumed to be 35 and 30 °C for Stockholm at the annual average ambient temperature of 5 °C, at which the heating demand is 65 kW. The water pump speed (i.e. mass flow rate) is assumed to be constant in the space heating loop and water forward temperature is assumed 45 °C at an ambient temperature of −18 °C. The CO_2 temperature exit from the space heating de-superheater follows the water return temperature with a 5 K approach temperature. These assumptions are adopted for the heat recovery discussion in Section 4.1.1. A simpler assumption of constant de-superheater exit temperature of 35 °C is adopted in other sections of the paper.

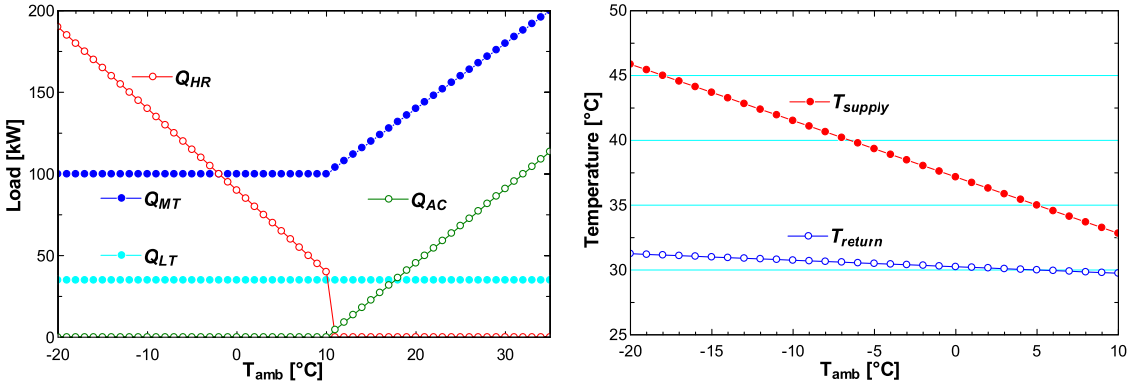

Fig. 4. Cooling and heating loads (left), Space heating water supply and return temperatures (right).

The air conditioning demand is estimated based on personal communication with the largest supermarket chain in Sweden. The supermarket chain has three typical sizes – small, medium and large – with a design AC capacity of 60, 100 and 200–250 kW, respectively. Similar ratios in AC load profiles corresponding to supermarket size have been adopted by Gullo et al. (2017). The medium-sized supermarket is selected for this study; the AC load is set to 100 kW at 32 °C and assumed to be zero at 10 °C. As shown in Fig. 1-right, the AC heat exchanger in the integrated CO_2 system is typically a flooded evaporator with two-phase flow CO_2 on one side of the plate heat exchanger and a water or secondary fluid loop on the other side. In this AC heat exchanger, water or secondary fluid is typically cooled down from 12 °C to 7 °C. As mentioned earlier, AC delivery is usually accompanied by the usage of parallel compression. Parallel compression is typically activated at ambient temperatures 10–15 °C; it is assumed to be activated in ambient temperatures higher than 13 °C in this paper, based on field measurements (Karampour and Sawalha, 2016b).

The assumed cooling and heating loads, and the water supply and return temperatures in the space heating loop are shown in Fig. 4. It is important to mention that some of these parameters are "indirectly" functions of outdoor ambient temperature, for example, the cooling and heating loads which are directly influenced by the indoor climate. Most of the other assumptions mentioned above are re-stated and summarised in Section 4 tables.

The high-pressure side of the refrigeration cycle is controlled based on summer floating condensing or winter heat recovery operation modes. When the ambient temperature is lower than 10 °C, the system runs in winter heat recovery mode. The heat recovery control strategy is explained in Section 4.1.1.

When the ambient temperature is higher than 10 °C, the system runs in floating condensing mode. The pressure of the gas cooler follows the ambient temperature in the sub-critical region with no sub-cooling, and 7 K approach temperature between the gas cooler exit temperature and ambient temperature. In the trans-critical region, the system runs at the optimum pressure for maximum COP. Eq. (1) shows the optimum pressure $P_{opt,gc}$ [bar] correlation as a function of the gas cooler exit temperature $T_{gc,exit}$ [°C] suggested by Sawalha (2008). This equation is developed based on finding maximum refrigeration COP for a range of gas cooler super-critical pressures versus a set of gas cooler exit temperatures. The units for the coefficients are 2.7 [°C /bar] and 6 [bar]. Approach temperature difference in trans-critical region is assumed to be 3 K.

$$P_{opt,gc} = 2.7 \times T_{gc,exit} - 6 \quad (1)$$

The approach temperature assumptions in sub-critical (7 K) and trans-critical (3 K) zones are based on the fact that the pinch point might be an issue in the sub-critical operation of the gas cooler, while it is of less importance in the trans-critical operation. The assumptions are made based on field measurement observations (Sawalha et al., 2017; Karampour and Sawalha, 2017), and also according to a discussion with a major manufacturer of air coolers and heat exchangers. As mentioned, the approach temperature in the de-superheaters is assumed to be 5 K.

As mentioned earlier, the cities used as samples of cold and warm climates in this modelling are Stockholm and Barcelona. Hourly ambient temperature data are extracted from Meteonorm as the average of years 2005–2015 (Meteotest, 2016). These hourly values are used to generate temperature-bin hour profiles, plotted in Fig. 5. It is worth mentioning that these two cities represent two regions in Europe with relatively cold and warm climates; it is speculated that the majority of European population is located within these two climatic cold and warm limits. However, the results for cities with more extreme climate conditions might be slightly different with the discussed results presented in Section 4.

3.2. Energy efficiency calculations

A computer model in EES (Engineering Equation Solver) software is used to analyse the performance of the CO_2 booster system (Klein, 2015). EES contains numerous built-in mathematical and thermo-physical property functions to give a numerical solution for a set of algebraic equations.

Mass flow rates in MT cabinets and LT freezers are calculated using the Eq. (2):

$$\dot{Q} = \dot{m}_{ref} \cdot \Delta h_{heat\ exchanger} \quad (2)$$

where $\dot{Q}$ [kW], as shown in Fig. 1-right, can be the cooling load in MT cabinets ($\dot{Q}_{MT}$) or LT freezers ($\dot{Q}_{LT}$). $\dot{m}_{ref}$ [kg s^{-1}] is the refrigerant mass flow rate and $\Delta h_{heat\ exchanger}$ [kJ kg^{-1}] is the enthalpy difference over the heat exchangers. The same equation is used to find the enthalpy differences over the de-superheaters, based on known tap-water heating ($\dot{Q}_{TWH}$) and space heating ($\dot{Q}_{SPH}$) demands. This will define the discharge pressure in the heat recovery mode, as explained later in Section 4.1.1. Energy–mass balances over the receiver and the assumed air conditioning demand ($\dot{Q}_{AC}$) are used to find the enthalpy and vapour quality change over the AC heat exchanger.

Knowing the mass flow rates in the different lines in the system, compressors electricity use $\dot{E}_{comp}$ [kW] in MT, LT and parallel compressor units are calculated using the below equation:

$$\dot{E}_{comp} = \left(\dot{m}_{ref} \cdot \Delta h_{is}\right)/\eta_{tot} \quad (3)$$

where η_{tot} is the overall efficiency of the compressors, and Δh_{is} [kJ kg^{-1}] is the isentropic enthalpy difference over each compressor unit. Compressors commercial datasheets are used to extract

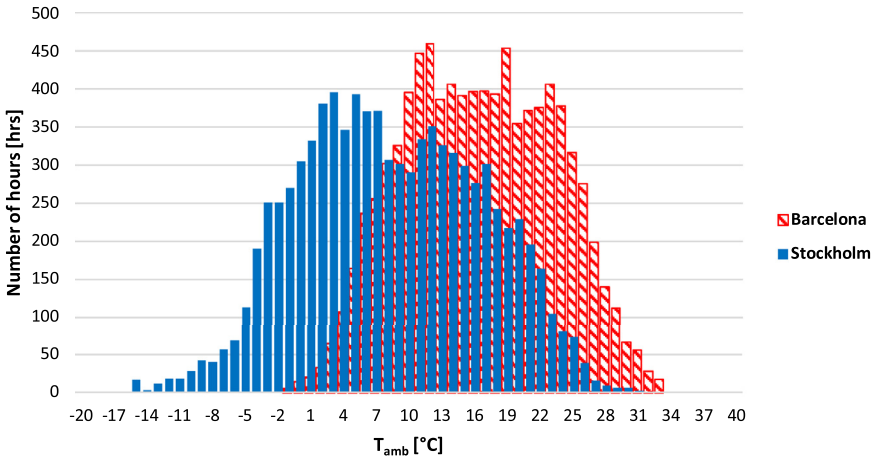

Fig. 5. Stockholm and Barcelona temperature-bin hour profiles, extract from Meteonorm (Meteotest, 2016).

the total efficiency of the compressors as a function of pressure ratios.

The total electricity use $\dot{E}_{tot}$ [kW] of the system is calculated based on the below equation

$$\dot{E}_{tot} = \dot{E}_{MT} + \dot{E}_{LT} + \dot{E}_{PC} + \dot{E}_{fan} \quad (4)$$

where $\dot{E}_{MT}$, $\dot{E}_{LT}$, and $\dot{E}_{PC}$ [kW] are the electricity use of three compressor units, shown in Fig. 1-right. $\dot{E}_{fan}$ [kW] is the electricity use of gas cooler fans. $\dot{E}_{fan}$ is estimated to be 3% of the heat rejected in the gas cooler $\dot{Q}_{gc}$ [kW], according to communication with a major CO_2 gas cooler manufacturer. This assumption has the same order of magnitude as in some other research works including Tsamos et al. (2017) and Lozza et al. (2007). This value is also assumed as 3% of gas cooler design capacity in Pack Calculation Pro software, which compares the annual energy use of different refrigeration systems (IPU, 2017).

The total refrigeration COP_{ref} [-] is defined as the ratio of total provided LT and MT refrigeration to the total electricity used "only" for the refrigeration function:

$$COP_{ref} = \left(\dot{Q}_{MT} + \dot{Q}_{LT}\right) / \dot{E}_{tot,only-refrigeration} \quad (5)$$

The calculation of COP_{ref} [-] for summer operation includes the power use only for refrigeration function; i.e. the estimated power consumed to provide AC ($\dot{E}_{AC}$ [kW]) is extracted from $\dot{E}_{tot}$. The parallel compressors are assumed to be large enough to compress all the vapours generated due to AC load and no vapour is expanded to MT level to be compressed by the high stage compressors. $\dot{E}_{AC}$ is found based on Eq. (3). COP_{AC} [-] is calculated using the following equation:

$$COP_{AC} = \dot{Q}_{AC} / \dot{E}_{AC} \quad (6)$$

To calculate COP_{ref} in winter operation and in order to eliminate the influence of heat recovery's extra electricity use, the system is assumed to run at 45 bar (about 10 °C), which is the minimum floating condensing temperature. CO_2 gas cooler minimum exit temperature is assumed to be 5 °C, to avoid frost formation on the gas cooler and oil circulation problems. At low temperatures, liquid CO_2 is heavier than the conventional lubricants, and there is a risk of oil build-up in the gas cooler. Furthermore, the oil becomes viscous at low ambient temperatures. The minimum condensation pressure and minimum gas cooler exit temperature are based on the field measurements observations and analysis which are presented in authors previous works (Sawalha et al., 2015; Karampour and Sawalha, 2016b).

Using this minimum floating condensing pressure, the power used for only-refrigeration function in winter operation is estimated. The difference between $\dot{E}_{tot}$ and $\dot{E}_{tot,only-refrigeration}$ is the power used for heat recovery $\dot{E}_{HR}$ [kW]. COP for heat recovery COP_{HR} [-] is calculated using the below equation

$$COP_{HR} = \left(\dot{Q}_{SPH} + \dot{Q}_{TWH}\right) / \dot{E}_{HR} \quad (7)$$

As explained earlier, the system's high-pressure side in the heat recovery operation mode is controlled for space heating. When the tap water heating is included in the calculations, it is considered as an extra space heating load; the discharge temperature is also checked to have proper values suitable for tap water heating. Separate COPs of tap water heating COP_{TWH}[-] and space heating COP_{SPH}[-] can be defined by finding the separate proportions of space heating and tap water heating loads in total electricity use; to fulfil this the electricity use is compared for the cases of "no heat recovery (only refrigeration)", "only space heating", and "both tap water and space heating".

The refrigeration COPs at MT and at LT levels, COP_{MT}[-] and COP_{LT}[-], are used to evaluate each function separately. The method of finding their electricity use proportions are explained in detail in a previous study by Karampour and Sawalha (2017). In brief, for COP_{LT}[-] calculation a proportion of electricity use by the MT compressors, which is due to low stage heat rejection (LT "condensing" load), is added to LT compressor electricity use. This high stage electricity use is deduced from the MT compressors electricity use while calculating COP_{MT}[-].

COPs are good indicators of energy efficiency performance as a function of temperatures. However, they do not provide sufficient information about the relative COP and time-dependent performance of different systems operating in different climates. In addition to COPs, standard and state-of-the-art CO_2 systems and other alternative cooling-heating solutions are compared using annual energy use AEU [MWh] and/or seasonal performance factor SPF [-]. These two indicators are calculated using the following equations:

$$AEU = \sum_{i=1}^{n} \left(\dot{E}_{tot,i} \cdot f_i\right) \quad (8)$$

$$SPF = \sum_{i=1}^{n} \left(\left[\frac{\dot{Q}_i}{\dot{E}_i}\right] \cdot f_i\right) \quad (9)$$

where n is the number of temperature-bin hours, and f is the frequency, i.e. number of hours, of each temperature bin. SPF can be calculated for different seasonal functions of the system, for example, heat recovery seasonal performance factor, SPF_{HR} [-], is used in this paper to compare the heat recovery function of the CO_2 system with that of other heating alternatives. The indicator for air

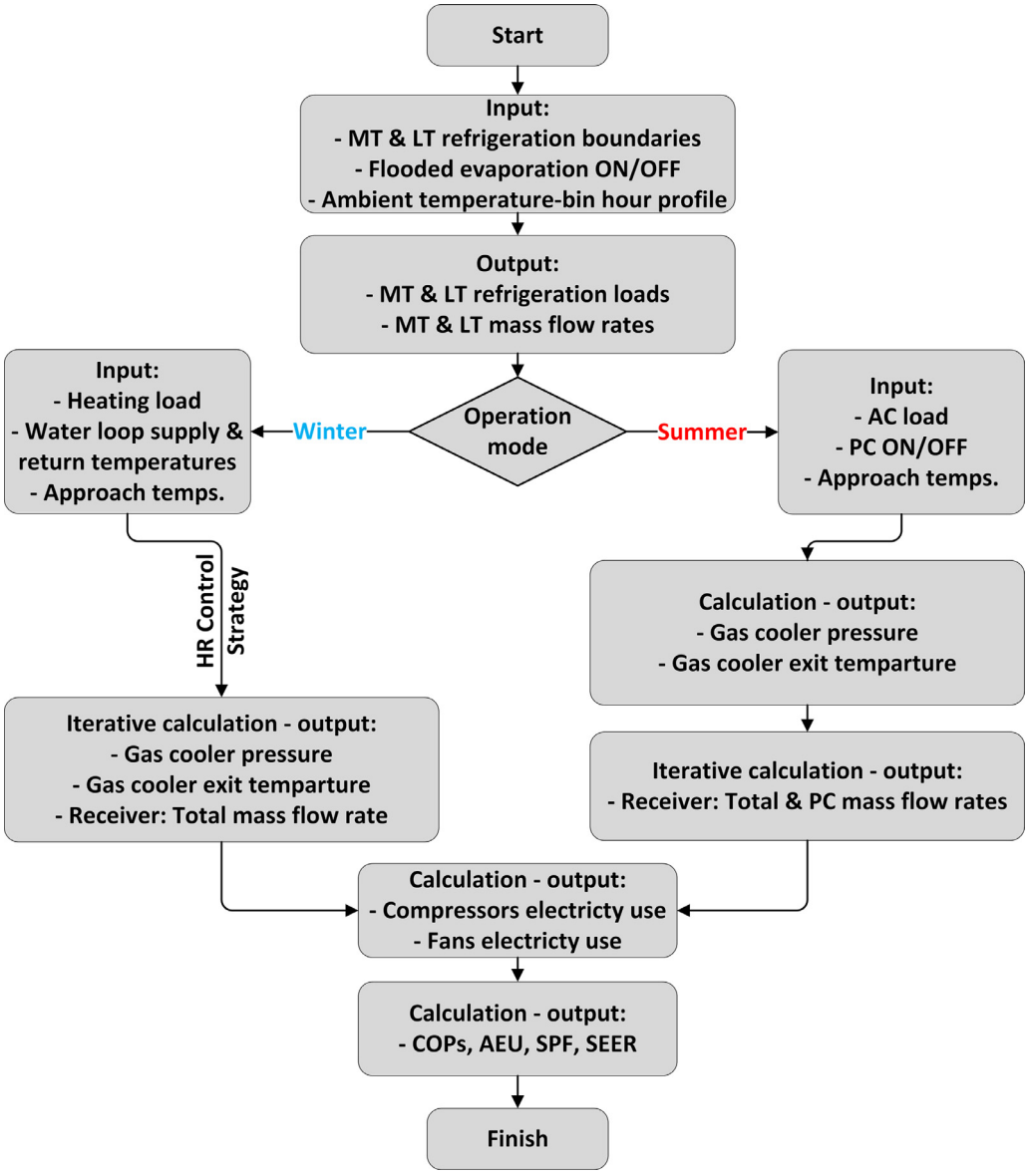

Fig. 6. Energy efficiency calculations flow diagram of the CO_2 system.

conditioning performance is conventionally called the Seasonal Energy Efficiency Rating/Ratio (SEER) according to the Eurovent standard OM-3-2017 (Eurovent, 2017). A simplified equation similar to Eq. (9) is used to calculate the air conditioning SEER, as shown in the below equation:

$$SEER = \sum_{i=1}^{n} \left(\left[\frac{\dot{Q}_{AC,i}}{\dot{E}_{AC,i}} \right] \cdot f_i \right) \tag{10}$$

The overall flow diagram of the CO_2 system energy efficiency calculations is presented in Fig. 6.

4. Results and discussion

The study of energy efficiency impacts of modified features and integrated functions in the CO_2 state-of-the-art system is presented in Section 4.1. The main modeling assumptions of this section are summarised in Table 1. The results of an energetic and environmental TEWI comparative analysis of various refrigeration system solutions are discussed in Section 4.2. The major modeling assumption for this section are summarised in Tables 2 and 3.

4.1. Evaluation of the features of state-of-the-art CO_2 system

4.1.1. Heat recovery

An essential feature of the state-of-the-art system is heat recovery. The heat is recovered in two de-superheaters to provide tap water heating and space heating. Usage of two de-superheaters instead of one gives better separated control of space heating and tap water heating functions. The authors' previous studies show that tap water heating is typically less than 10–15% of the total heating demand (Karampour and Sawalha, 2017), and the system heat recovery control is assumed to be governed by the space heating demand.

The heat recovery start set point is at 10 °C ambient temperature. System control in heat recovery mode is modelled based on Sawalha (2013) heat recovery control strategy. In brief, the recommendation consists of a stepwise control strategy; the first step is to regulate the gas cooler pressure P_{gc} and keep the gas cooler exit temperature $T_{gc,exit}$ as low as possible (minimum 5 °C) by running the gas cooler at full capacity. The second step is to fix the gas cooler pressure at a maximum value

Table 1
Assumptions and boundary conditions used in modelling of the state-of-the-art features.

System/parameter	Assumed values	Notes
4.1.1 Heat recovery		
CO_2 heat recovery	Heat recovery set point @ $T_{amb} = 10$ °C, 40 kW heating load	Based on CyberMart modeling (Arias, 2005) and field measurement observations (Karampour and Sawalha, 2016a,b)
	Minimum gas cooler pressure: 45 bar Minimum gas cooler exit temperature: 5 °C Design condition (I): 65 kW @ $T_{amb} = 5$ °C, Water $T_{supply} = 35$ °C, $T_{return} = 30$ °C Design condition (II): 180 kW @ $T_{amb} = -18$ °C, Water $T_{supply} = 45$ °C	
Air source heat pump (ASHP)	Refrigerant: R407C Internal super-heating: 10 K Evaporator approach temperature: 7 K Minimum evaporation temperature: −15 °C Auxiliary electric heater cut-in @ $T_{amb} = -5$ °C Auxiliary heater full capacity: 180 kW @ $T_{amb} = -18$ °C Auxiliary heater efficiency: 95% Defrosting electricity use ratio to compressors: 7%	
4.1.2 Flooded evaporation		
CO_2 standard and CO_2 SotA systems	CO_2 standard (DX)	Based on modeling in IMST-Art software (IMST-ART, 2017),
	• $T_{MT} = -8$ °C • $T_{LT} = -32$ °C	A 5 kW MT cabinet cooling air from 8 °C to 3 °C A 3.5 kW LT freezer cooling air from −20 °C to −24 °C
	• 10 K internal super-heating CO_2 SotA (Flooded) • $T_{MT} = -4.3$ °C • $T_{LT} = -29$ °C • 0 K internal super-heating (saturated vapour)	
4.1.3 Parallel compression and Air conditioning		
Parallel compression vs Flash gas by-pass	CO_2 standard: • Flash gas by-pass CO_2 SotA: • Parallel compression activated for T_{amb} higher than 13 °C	
CO_2 Air conditioning	AC start set point @ $T_{amb} = 10$ °C, 0 kW AC load Design AC load: 100 kW @ $T_{amb} = 32$ °C Evaporation temperature: 1.5 °C, saturation temperature corresponding to the receiver pressure	
HFC Air conditioning	Refrigerant: R410A Evaporation temperature: 0 °C Internal super-heating: 10 K Condenser approach temperature: 7 K	
4.1.4 Other state-of-the-art features		
Mechanical sub-cooling	Start set point @ $T_{amb} = 15$ °C Refrigerant: Propane R290 Design capacity: 30–60 kW for sub-critical @ T_{amb} varies 15–23 °C, fixed 60 kW for trans-critical pressures Sub-cooling in propane loop: 0 K Internal super-heating: 5 K Evaporation temperature: 0 °C Condenser approach temperature: 7 K Condenser fans electricity use: 3% of gas cooler heat rejection load	Based on modeling an R290 mechanical sub-cooler providing 15–20 K sub- or further-cooling.
Gas cooler evaporative cooling	Start set point @ $T_{amb} = 25$ °C Evaporative cooling process efficiency: 80%	Partly based on Lozza et al. (2007) Partly based on Girotto and Minetto (2008)
LT de-superheater	LT de-superheat exit temperature in “summer heat rejection” and “winter heat recovery”: 35 °C	Similar to high stage space heating de-superheater

$P_{gc,max}$ and decrease the gas cooler capacity by reducing the fans speed or, ultimately, by-passing the gas cooler using the by-pass valve. $P_{gc,max}$ can be calculated using Eq. (1) but using the 2nd de-superheater exit temperature instead of gas cooler exit temperature.

The heat recovery from the CO_2 system is compared with a separate HFC-based heat pump. In this comparison, an air source heat pump (ASHP) is considered, because ambient temperatures between 10 and −5 °C occur in 85% of the winter time in Stockholm, where ASHP has comparable energy efficiency to a ground source heat pump (GSHP). This has been evaluated calculating the heating performance for ASHP and GSHP systems.

The evaporators of the CO_2 system are assumed to be flooded, and the evaporation temperatures at MT and LT level are assumed to be 3–4 K higher than the CO_2 standard system, −4.3 and −29 °C compared to −8 and −32 °C. Possible methods of providing these higher evaporation temperatures are explained in Section 4.1.2.

R407C (GWP = 1774) and R410A (GWP = 2088) are two refrigerants used widely in heap pumps. The modelled air–water ASHP uses R407C as the refrigerant and a compressor total efficiency correlation is developed based on a commercial product (BITZER, 2017). 10 K of internal super-heating is assumed at the suction of the compressor. The approach temperature in the evaporator is 7 K, and the minimum evaporation temperature is −15 °C.

Table 2
Assumptions and boundary conditions used in modelling of the studied refrigeration systems.

Parameter	Assumed value	Notes
Medium stage evaporation temperature	-8 °C for: • CO_2 standard • HFC/HFO DX and indirect • NH_3 and propane units in cascade systems -4.3 °C for: • CO_2 SotA • CO_2 in Cascade systems	
Low stage evaporation temperature	-32 °C for: • CO_2 standard • HFC/HFO DX and indirect -29 °C for: • CO_2 SotA • Cascade	
Minimum condensation temperature	10 °C for: • CO_2 standard • CO_2 SotA • HFC/HFO DX 15 °C for: • Cascade • HFC/HFO indirect	10 °C in air-cooled condensers/gas coolers and 15 °C in secondary fluid-cooled condensers. This will keep the minimum temperature at the exit of the condenser or dry-cooler at 5 °C.
Condenser/gas cooler approach temperature and sub-cooling	3 K for: • CO_2 standard in trans-critical • CO_2 SotA in trans-critical 7 K for: • CO_2 standard in sub-critical • CO_2 SotA in sub-critical • HFC/HFO DX 5 K for: • HFC/HFO indirect condenser • HFC/HFO indirect dry cooler • Cascades in condenser • Cascades in dry cooler No sub-cooling for any system 5 °C minimum gas cooler (CO_2), condenser (DX) and dry cooler (indirect-cascade) exit temperature	5 K in liquid-cooled condensers, and dry coolers 7 K in sub-critical air-cooled condenser 3 K in trans-critical CO_2 gas cooler
Evaporator internal super-heating	• 10 K for DX evaporators • 0 K for flooded evaporators • 8 K after IHX for NH_3 and propane	
External super-heating	• 10 K for all MT and LT loops passing the sales area • 0 K for NH_3 and propane loops • 0 K HFC/HFO indirect MT stage	No external super-heating is considered for evaporators in the machinery room.
Compressors efficiencies	As a function of pressure ratios, developed by using manufacturers data, all semi-hermetic compressors, NH_3 open type compressor	All the compressors have total efficiencies in the ranges of 60–65% for LT and 65–70% for MT and high stage in cascades
Auxiliary powers	• Fans power: 3% of the air-cooled condenser/gas cooler load in all systems. • HFC/HFO indirect: pumps power 20% of compressors power. • Cascade: CO_2 and secondary fluid pump powers calculated.	Fan power according to communication with a major gas cooler/condenser manufacturer. HFC indirect pump power according to field measurements presented by Sawalha et al. (2017).

For ambient temperature between −5 and −10 °C, the heating capacity of ASHP is fixed as a maximum, and the remaining heat required is provided by an auxiliary electric heater. Evaporator electric defrosting power is considered as 7% of compressor power in the below 0 °C region. When the ambient temperature is lower than −10 °C, ASHP is switched off and the auxiliary electric heater with 95% efficiency provides the required heating demand. The auxiliary heater is switched on at −5 °C T_{amb}, and its capacity can increase up to 180 kW at −18 °C T_{amb}.

Heating COPs and SPF of CO_2 heat recovery and ASHP are shown in Fig. 7. As can be seen in the graph, COP_{ASHP} is often higher than COP_{HR} at ambient temperatures above 0 °C. However, COP_{HR} has significantly higher values at ambient temperatures lower than 0 °C. These higher COP values are reflected in about 10% higher SPF_{HR} of CO_2 system (SPF_{HR}=3.9) compared to ASHP system (SPF_{ASHP}=3.6). It is necessary to mention that if the system is located in warmer climates, for example Barcelona, or if the heat recovery is activated at higher ambient temperatures, for example 15 °C, the running situations is in favour of air source heat pumps and it is expected that they have higher SPF than CO_2 heat recovery.

In addition to the 10% higher SPF_{HR} value, heat recovery from the CO_2 system is significantly more compact heating solution; the only added components are one or two compact plate heat ex-

Table 3
TEWI analysis assumptions.

Parameter	Assumed value	Notes
Leakage rate [%]	10% DX loops 5% indirect loops	$M_{leakage}$ divided by M_{ref} [%]
***N* [years]**	15 years	
Refrigerant charge [kg/kW]	CO_2: MT = 3, LT = 3	Charge of refrigerant per design capacity of refrigeration unit
	Cascade: high stage = 0.75 (compact units)	Values are partly adopted from Emerson Climate Technologies (2010)
	Cascade: low stage = 4 HFC/HFO DX: MT = 2, LT = 4 HFC/HFO indirect: MT = 1, LT = 3	
Design refrigeration capacity [kW]	200 kW for MT, 250 kW for cascade high stage evaporators, 35 kW for LT	Design temperature 35 °C T_{amb}
κ	0.95	
GWP_{ref}	CO_2 = 1, NH_3 (R717) = 0, Propane (R290) = 3, R404A = 3922, R449A = 1397	(BITZER, 2016)
RC [$kgCO_2/kWh_{el}$]	Sweden = 0.079 Spain = 0.639	(Bertoldi et al., 2010)

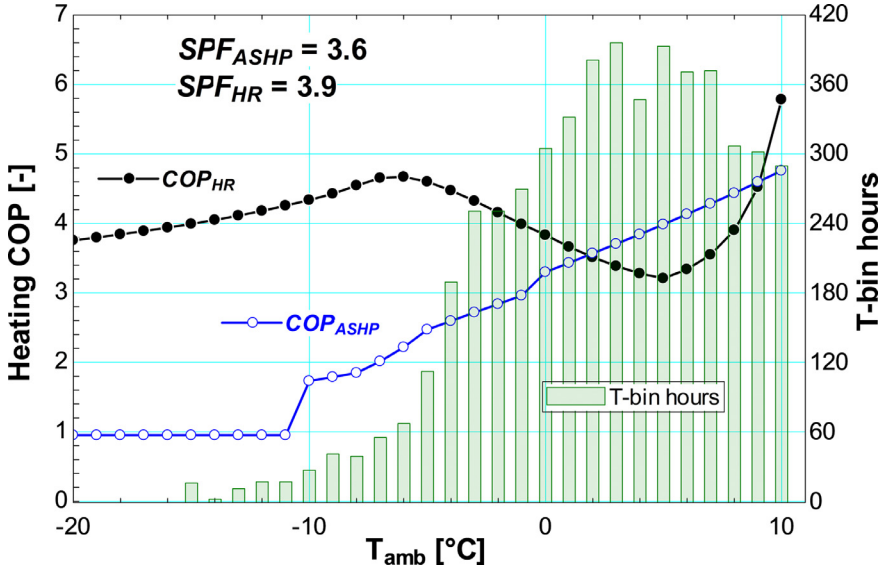

Fig. 7. Heating COP and SPF of CO_2 heat recovery and ASHP. On the right axis is Stockholm winter temperature-bin hour.

changers as de-superheater, compared to a stand-alone ASHP unit and an auxiliary electric heater. Furthermore, there is no limitation in low ambient temperature operation, and it uses a refrigerant with no environmental short- or long-term concerns. Compared to HFC heat pumps, the CO_2 system can also provide a greater amount of high-grade heat proper for the high temperature demands of tap water heating.

20–45% of the recovered heat from the CO_2 system in + 10 to −20 °C T_{amb} range is high-grade heat; i.e. it has CO_2 temperatures higher than 65 °C, suitable to provide tap water heating demand with a temperature of 55–60 °C. Tap water heating demand is provided almost for free in summer time, due to high CO_2 discharge temperatures in the floating condensing mode; i.e. there is no need to raise the discharge pressure. In order to calculate the tap water heating COP in winter, an hourly model is used instead of the temperature-bin model. Tap water heating demand is assumed as being 15 kW, supplied two hours early in the morning for food preparation and two hours late at night during supermarket cleaning. The assumptions regarding these operations are based on the observed hot water consumption pattern in a supermarket. The calculated average COP value for tap water heating is 5.4 which shows that the tap water heating function of the CO_2 system is a very energy efficient solution for providing hot water.

The total energy costs of CO_2 heat recovery and ASHP are compared to another conventional heating alternative, the district heating. The total space heating demand which is provided by any of these three systems is about 410 MWh, this number is based on the load assumptions presented before. It is assumed that district heating can provide the entire space heating demand at the required temperature. The electricity price is assumed as 0.1 €.kWh^{-1} for electricity and 0.05 €.kWh^{-1} for district heating. As can be seen in Fig. 8, the total energy cost of CO_2 heat recovery is about 50% less than for district heating, and 20% less than ASHP.

4.1.2. Flooded evaporation

In order to evaluate the impact of flooded evaporation in raising the evaporation temperature, the evaporators of an average size MT cabinet and an average size LT freezer are modelled in IMST-ART software. IMST-ART is a software developed at the Polytechnic University of Valencia, able to integrate a set of models for every component of a vapour compression cycle to analyse the performance of individual components and the system (IMST-ART, 2017). The MT cabinet size is assumed to have 5 kW capacity and it is supposed to cool the air from 8 °C to 3 °C, by a CO_2 evaporation temperature of −8 °C and 10 K internal super-heating. By removing the 10 K super-heat and keeping evaporator capacity and air side temperatures constant, the evaporation temperature can be raised

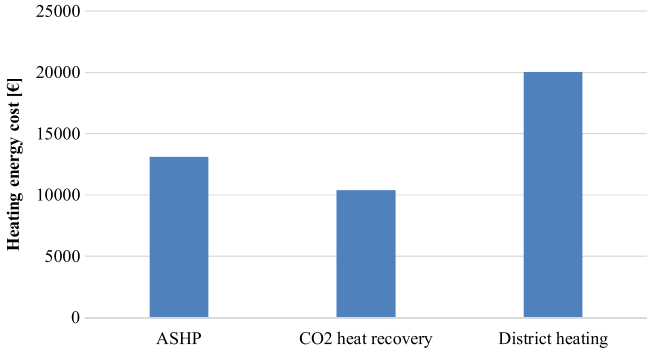

Fig. 8. Annual heating energy cost of three heating systems [euros].

to −4.3 °C (3.7 K increase from −8 °C in the standard system). This way the CO_2 leaves the evaporator at saturated vapour condition. The same procedure is carried out in order to model a 3.5 kW LT freezer cooling the air from −20 °C to −24 °C by CO_2 evaporating at −32 °C and 10 K internal super-heating. The results show that the system can be run at −29 °C evaporation temperature (3 K increase from −32 °C in the standard system) and no super-heat. The higher evaporation temperature due to flooded evaporation results in less defrosting demand, compared to the standard system. This positive impact of the flooded evaporation is not considered in the AEU comparison.

The calculations show that the MT evaporation temperature increase results in 9% AEU saving in Stockholm and 10% in Barcelona. Raising the LT evaporation by 3 K will save about 2–3% AEU in both cities. The savings for flooded LT is insignificant due to the large load ratio LR ($\dot{Q}_{MT}/\dot{Q}_{LT}$). The AEU savings for flooded LT will be higher in systems with lower load ratio.

The combined effect of running MT and LT in flooded case is an AEU saving of about 12% in Stockholm and Barcelona, compared to the standard CO_2 booster system with heat recovery. These results are summarised among other features in Fig. 11.

Three methods which can be implemented in order to flood the MT and/or LT evaporators are discussed in the following paragraphs.

The first method to run the system with flooded evaporators is to use a single or a set of ejectors. A simple schematic of such a system is shown in Fig. 9a. The ejector is used to return the liquid collected after the MT evaporators, from the liquid accumulator to the receiver. The cabinet expansion valve is controlled by the air return temperature instead of the super-heating amount. Ejectors have the possibility of running both MT and LT levels in flooded evaporation mode with a set of ejectors. This is described in several publications, such as Hafner et al. (2014), Minetto et al. (2014a) and Gullo et al. (2017). The description of some field installations using ejector for flooded evaporation can be found in Hafner et al. (2016), Schönenberger et al. (2014) and Minetto et al. (2014b).

The second method is using a pump circulation unit, as shown in Fig. 9b. The pump directs the accumulated liquid after the MT evaporators back to the receiver. The pump should be actuated by a liquid switch in the accumulator tank. Usage of pump circulation for flooded evaporation has already been implemented in full CO_2-based ice rink refrigeration systems (Rogstam and Bolteau, 2016; Rogstam, 2016; Simard, 2012). Pump circulation in cascade ammonia–CO_2 systems has also been applied in supermarkets (Knudsen and Pachai, 2004), supermarket laboratory experiments (Sawalha et al., 2007) and ice rinks (Nilsson et al., 2007). Similar to the ejector solution, the oil trapped in the accumulator and the receiver should be directed back to the compressors' suction line using an oil separation and return mechanism. As an example, this oil separation technique is used in the first European ice rink using only CO_2 as the refrigerant (Rogstam and Bolteau, 2016). The CO_2 pump electricity use is calculated and added to the compressors and gas cooler fans electricity use. It is assumed that the pump compensates for 70 kPa pressure drop, its efficiency is equal to 70% and the circulation ratio is 2. The latter means that the mass flow rate of refrigerant in the evaporators is twice as much the rate needed to achieve full evaporation. The calculations show this AEU saving is about 1% lower compared to the ejector solution for an efficient pump with 70% efficiency and low pressure drop of 70 kPa. The AEU saving is about 2% lower compared to the ejector solution for an inefficient pump with 40% efficiency and high pressure drop of 400 kPa. The CO_2 pump power is in both cases insignificant compared to the compressor power.

The third method which can be applied is by using internal heat exchangers (IHX) inside the cabinets, and the way how this is done in LT cabinets is shown in Fig. 9c. The signal to the expansion valve is sent from the CO_2 stream exiting the IHX, instead of the traditional internal super-heating control. In this case, all, or most, of the super-heating is achieved inside the IHX instead of inside the evaporator. This flooded evaporation solution and its challenges are elaborated more in some other research works including (Tambovtsev and Quack, 2007).

In all the three methods presented for flooded evaporation, it is important that the gas cooler and receiver be sized properly to be sure that the system (evaporators) is always provided with the required amount of liquid CO_2.

4.1.3. Parallel compression and air conditioning

Parallel compression (PC), as shown in Fig. 1-right, is an alternative method to direct the vapour formed in the receiver back to the high-pressure side. It is more efficient than the standard flash gas by-pass applied in standard systems since it compresses the vapour from higher suction pressures compared to MT compressors. The main limitation to using PC is the minimum flow rate restriction of the parallel compressors. There should be a minimum vapour content in the receiver to actuate the parallel compression and more vapour in the receiver is a more favourable condition to run PC. The minimum flow rate which the parallel compression unit can handle is equal to the smallest flow rate corresponding to the PC lowest capacity in part load operation.

According to observations from a supermarket in Sweden (Karampour and Sawalha, 2016b) and other research such as Javerschek et al. (2015), PC is typically activated when T_{amb} is higher than 10–15 °C; therefore, 13 °C is assumed to be as the set point for PC activation in this analysis. The calculations show that using PC can save about 3% AEU in Stockholm and about 7% in Barcelona compared to a standard CO_2 system with flash gas by-pass.

Air conditioning (AC) integration into the CO_2 system is another feature of the state-of-the-art system. It is a compact solution that requires the addition of few extra components in contrast to a stand-alone AC unit. Another advantage is that the refrigerant is CO_2, while stand-alone AC units are typically HFC or HFC/HFO based and are often subject to environmental regulations and restrictions. AC demand matches well with PC running conditions; AC demand increases as the ambient temperature increases, and this will generate more vapour in the receiver and extend the running hours of PC. Therefore, AC with PC is considered as a feature of the CO_2 state-of-the-art system.

The AC performance of a CO_2 state-of-the-art system is compared to a conventional stand-alone AC system using R410A (GWP = 2088) as the refrigerant. The R410A system has an evaporation temperature of 0 °C, and the approach temperature difference on the condenser side is 7 K, similar to CO_2 sub-critical air-cooled condensation. The AC seasonal energy efficiency ratio

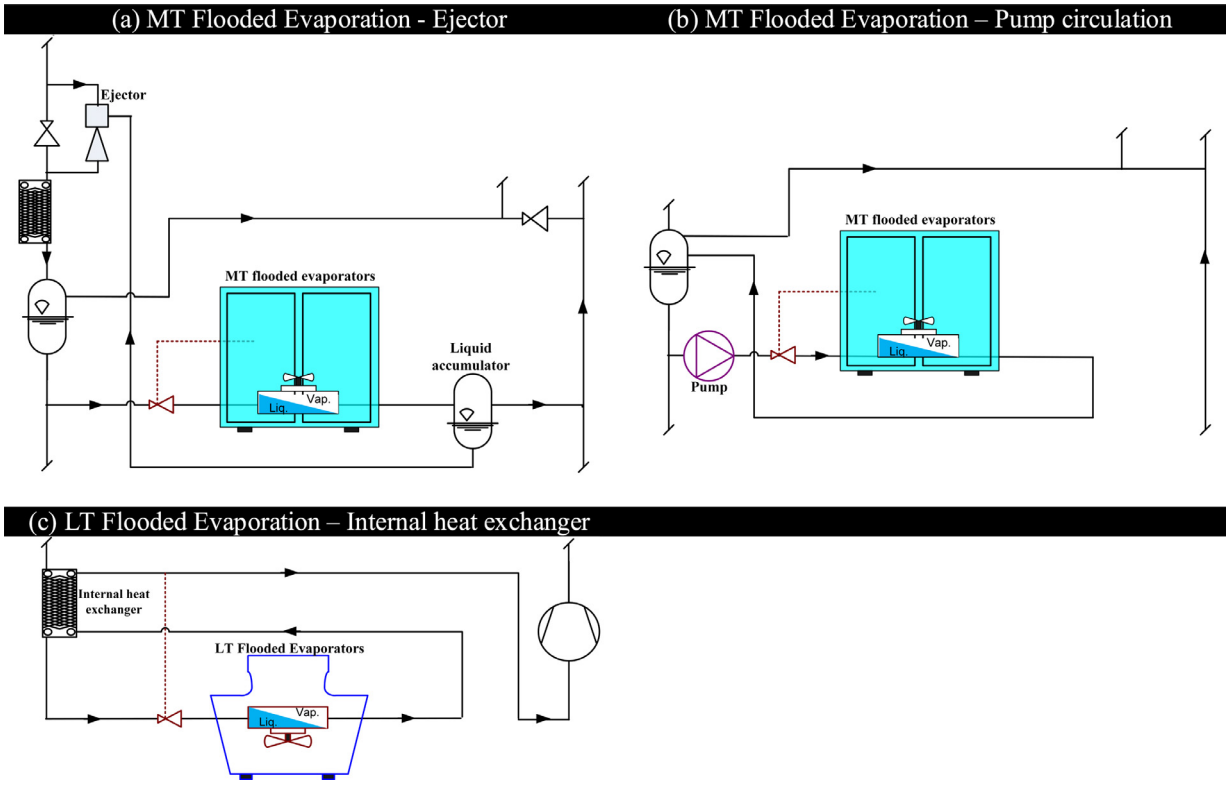

Fig. 9. Schematic diagram of methods of providing flooded evaporation: a) Ejector, b) Pump circulation and c) IHX.

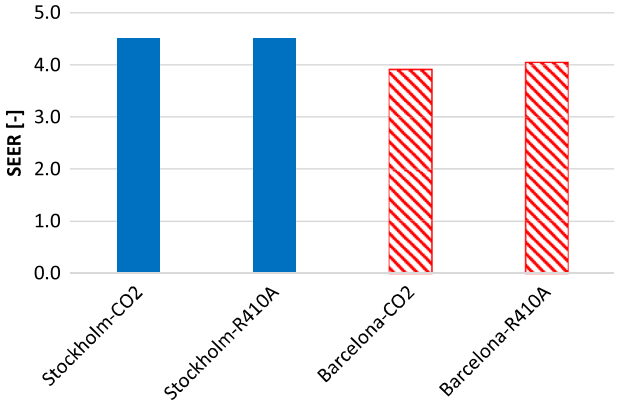

Fig. 10. Seasonal Energy Efficiency Ratio $SEER_{AC}$ of CO_2 and R410A AC solutions in Stockholm and Barcelona.

SEER [-] of these two systems is calculated using Eq. (10); it is the temperature-bin weighted average of air conditioning load $\dot{Q}_{AC}$ over AC electricity use $\dot{E}_{AC}$. The comparison result is shown in Fig. 10. As can be observed, $SEER_{AC,\ CO2}$ is comparable to $SEER_{AC,\ R410A}$ in Stockholm (about 4.5) and in Barcelona (about 4.0). Other economic factors worth mentioning include: saving space, being an environmentally friendly long-term solution, requiring fewer components and less refrigerant (compared to a complete stand-alone system).

An assumption made in the AC calculations is the starting set point temperature of 10 °C. This value is based on observations and field measurements analysis of Swedish supermarkets. It is speculated that specific thermal zones in the supermarket, for example bakery, have lower AC set point values than the typical room AC set points. However, this assumption does not influence the result significantly since the AC load is very small in these low ambient temperature ranges. If the AC start set point is assumed as, for example, 20 °C, the situation is in favour of R410A AC systems.

4.1.4. Other state-of-the-art features

There are other modifications which have less significant impacts (as the analysis following will show) or more application limitations compared to the key features of the state-of-the-art system, which are analysed in the previous sub-sections.

Mechanical sub-cooling: sub-cooling has a positive impact on the refrigeration performance. An external mechanical sub-cooler using natural refrigerant propane is a solution recently implemented in some warm climate CO_2 system installations (Frigo-Consulting, 2014; Advansor, 2015). A propane mechanical sub-cooler is modelled and designed to increase its capacity linearly between 30–60 kW in sub-critical conditions of ambient temperatures between 15–23 °C. It is run with full capacity, i.e. 60 kW, in trans-critical conditions. These capacity values are based on a calculation to size a sub-cooler to provide a reasonable 15–20 K sub- /further-cooling. The propane sub-cooler cycle operates as a simple refrigeration cycle with no sub-cooling and 5 K internal super-heating. Propane evaporation temperature is set to 0 °C, and the condensing temperature has 7 K approach difference with T_{amb}. Condenser fan power use is set to be 3% of the condenser heat rejection amount.

AEU saving has been studied for 15 °C T_{amb} starting set point of mechanical sub-cooling, and it is found that about 3% in Stockholm and 7.6% in Barcelona can be saved. However, the set point for using mechanical sub-cooling is typically higher than 15 °C (Frigo-Consulting, 2014), which reduces the expected energy savings presented in this study. The investment cost of a 60 kW propane sub-cooling unit should be taken into account which might be a strong factor in limiting the application of this feature. It is recommended to consider this feature as an arbitrary feature for moderate and warm climates, but it can be considered as a strong option in very warm climates. The calculations in the design stage could prove its applicability and duration of application. Furthermore, usage of

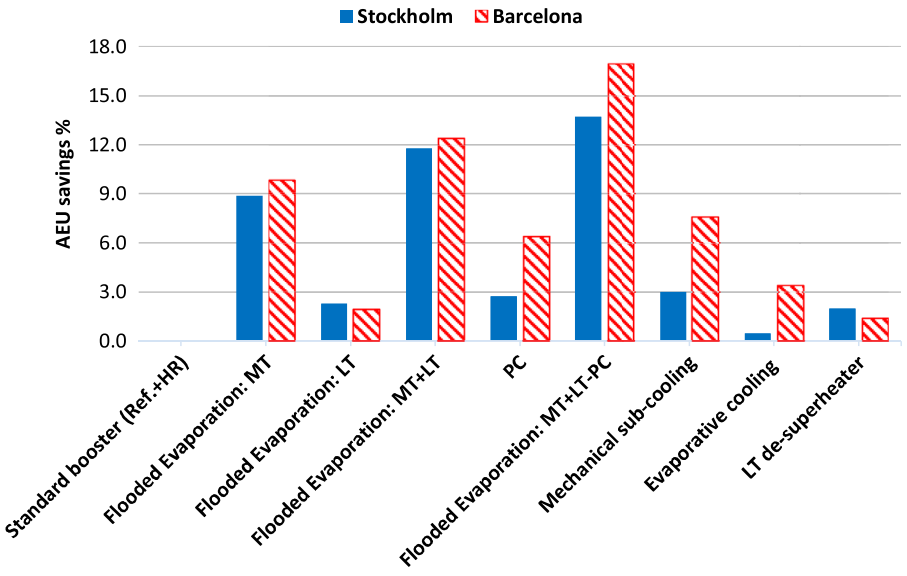

Fig. 11. Impacts of modifications on AEU compared to a "standard CO_2 booster with heat recovery".

mechanical sub-cooling can reduce the running hours of parallel compression. These interactions should also be taken into account in the design stage.

Gas cooler evaporative cooling: in order to avoid operating the refrigeration system at high trans-critical pressures, water can be sprayed in the inlet air stream to the gas cooler. The evaporative cooling is activated when the outdoor temperature is relatively high. In this modelling work, the evaporative cooling is activated at an ambient temperature of 25 °C and above. The evaporative cooling process is assumed to be 80% efficient. 100% evaporative cooling efficiency means the dry bulb temperature reaches the wet bulb temperature. This evaporative cooling process results in lowering the dry bulb temperature by about 3 K, considering the relative humidity data extracted from Meteonorm (Meteotest, 2016).

It is calculated that the AEU saving is 1% in Stockholm and 3% in Barcelona. The main reason for this negligible impact is the running hours of evaporative cooling; it is active only for 2% of the year in Stockholm and 14% in Barcelona, referring to Fig. 5. Barcelona has relatively humid summer season. Evaporative cooling could result in higher annual savings in cities with drier summer periods. However, availability of water, water treatment, and components corrosion are some other factors which could limit the feasibility and wide spread usage of this choice.

LT de-superheater: a de-superheater after the LT booster compressor can be used for heat recovery in winter time and heat rejection in summer time. In both seasons, a simple assumption is used where the de-superheater is assumed to cool CO_2 down to 35 °C. The annual calculations of the system performance show that AEU saving is insignificant, less than 2% in case of using LT de-superheater. The reason for this insignificant saving is that the low stage mass flow rate in the LT is considerably smaller compared with high stage mass flow rate. This is due to the higher refrigeration load at MT than LT. In winter, the heat recovery ratio of low stage unit (the recovered heat in the low stage de-superheater divided by the LT refrigeration load) is about 7%, corresponding to 3 kW only.

4.1.5. Comparison results

The results of all the discussed modifications impact on AEU saving [%] are summarised in Fig. 11. The reference system is a standard CO_2 booster system with heat recovery. Heat recovery is included in all the modified solutions while air conditioning is not included. According to the results, the combined effect of flooded evaporation in MT and LT levels and parallel compression shows the most promising solution which saves 13 and 17% of AEU in Stockholm and Barcelona, respectively.

Considering the discussed results in these five sub-sections, the state-of-the-art CO_2 refrigeration system (SotA) can be defined as a system integrating heating and air conditioning functions. It uses flooded evaporation in MT and LT level, and parallel compression due to the significant combined effects of these features on energy efficiency. Mechanical sub-cooling, gas cooler evaporative cooling and LT de-superheater are not considered as essential features of this state-of-the-art system. However, for the regions with much warmer and drier climate conditions than Barcelona, mechanical sub-cooling and evaporative cooling are worth to be evaluated in the system design procedure.

In addition to the energy saving comparisons, an economic calculation is done to find out how much would it be justified to pay for each modified feature in order to get higher system efficiency. The lifetime of the system is assumed 15 years and the electricity price 0.1 €.kWh^{-1}. The results of this "justified cost" economic calculation is shown in Fig. 12. As can be seen, the most efficient solution, combined flooded MT-LT and PC, justifies the payment of 104 thousand euros in Stockholm and 156 thousand euros in Barcelona.

Integration of heat recovery and air conditioning in the SotA system are other important features when comparing the installation cost of CO_2 and other alternative cooling-heating solutions. These functions integration into the CO_2 refrigeration system has much less installation cost comparing to conventional stand-alone heating and air conditioning systems.

4.2. Comparison of the state-of-the-art system with alternative refrigeration systems

The performance of state-of-the-art CO_2 system is compared to standard CO_2 and key alternative refrigeration solutions. These alternative systems include: conventional direct expansion DX, indirect synthetic refrigerant-based systems, and natural refrigerant-based cascade solutions. These systems are described in Section 2. The main assumptions for the comparison are summarised in Table 2.

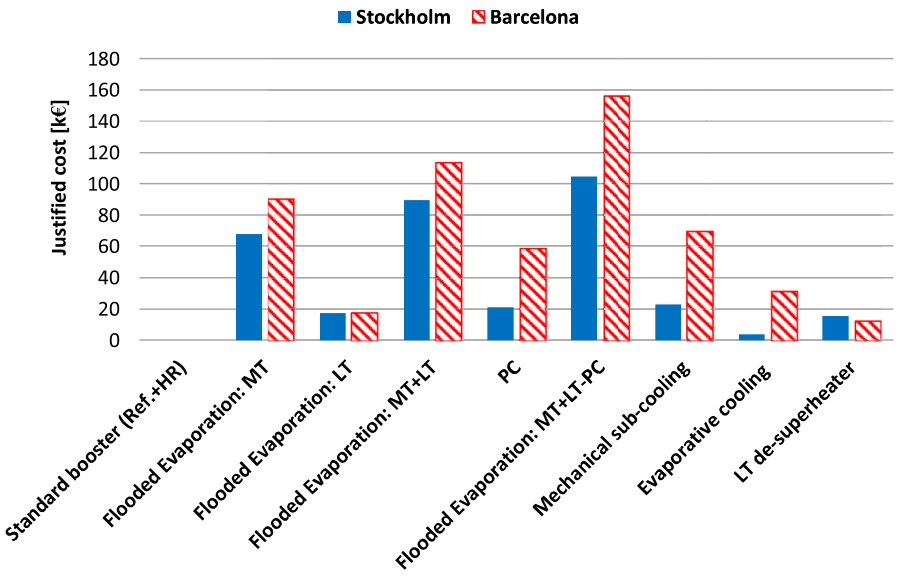

Fig. 12. Justified cost [thousand Euros] for implemented modifications.

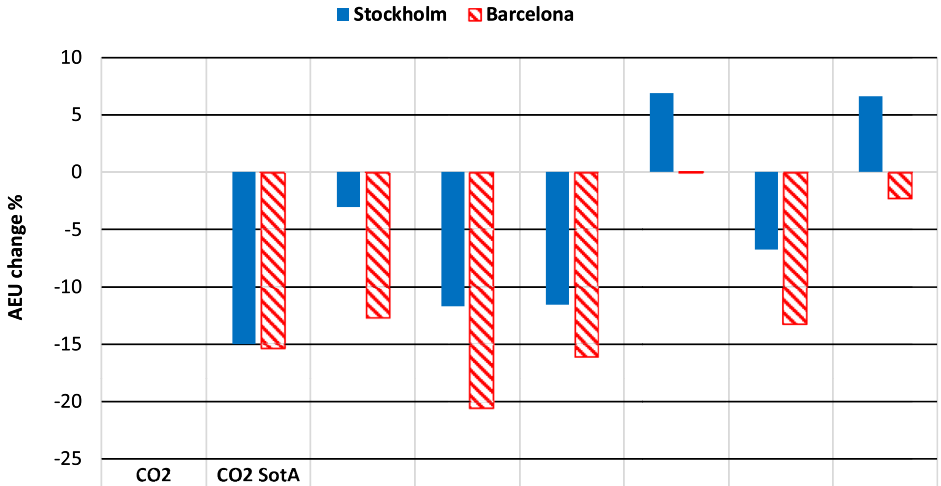

	CO2 standard booster (ref.)	CO2 SotA (PC+flooded MT&LT)	Cascade R290-CO2	Cascade NH3-CO2	R404A DX	R404A Indirect	R449A DX	R449A Indirect
Stockholm	0.0	-15.0	-3.1	-11.7	-11.6	6.9	-6.8	6.6
Barcelona	0.0	-15.4	-12.8	-20.6	-16.2	0.0	-13.3	-2.3

Fig. 13. Annual Electricity Use (AEU) change % compared to reference CO_2 standard system (only refrigeration load is included, no heat recovery).

4.2.1. Comparison results and discussion

The annual electricity use AEU of the refrigeration systems are compared to the reference standard CO_2 trans-critical booster system in Stockholm and Barcelona. Only refrigeration load is included in this comparison. The annual electricity use of this system is 425 MWh in Stockholm and 612 MWh in Barcelona. The results of the comparison are shown in Fig. 13. The negative values indicate the percentage of energy saving compared to the reference system.

State-of-the-art CO_2 system is the most energy efficient refrigeration solution in Stockholm, saves 15% of AEU compared to the standard CO_2 system. Ammonia–CO_2 cascade and R404A DX have comparable savings of about 12% in Stockholm and R449AA DX system saves about 7% of AEU.

The most energy efficient solution in Barcelona is ammonia–CO_2 cascade with 21% AEU saving. CO_2 SotA and R404A DX have comparable savings of 15–16% and R449AA DX system saves about 13% of AEU. The CO_2 SotA system is still a strong solution considering the limitations of other alternative refrigeration system, discussed later in this section.

Propane–CO_2 cascade solution has about 9% less saving compared to ammonia–CO_2 cascade solution in both cities. The main reason for this difference is compressors efficiencies. The selected commercial propane compressor has about 5% less efficiency compared to the ammonia compressor. With a more efficient propane compressor this gap will decrease.

The HFC/HFO indirect solutions have the least efficiency in both cities. In a previous study, it is calculated that standard CO_2 refrigeration system is about 12% more efficient than R404A indirect system (Karampour and Sawalha, 2017). This difference is reduced to about 7% in this study. The main reason for this is slight changes in the assumptions including the approach temperatures.

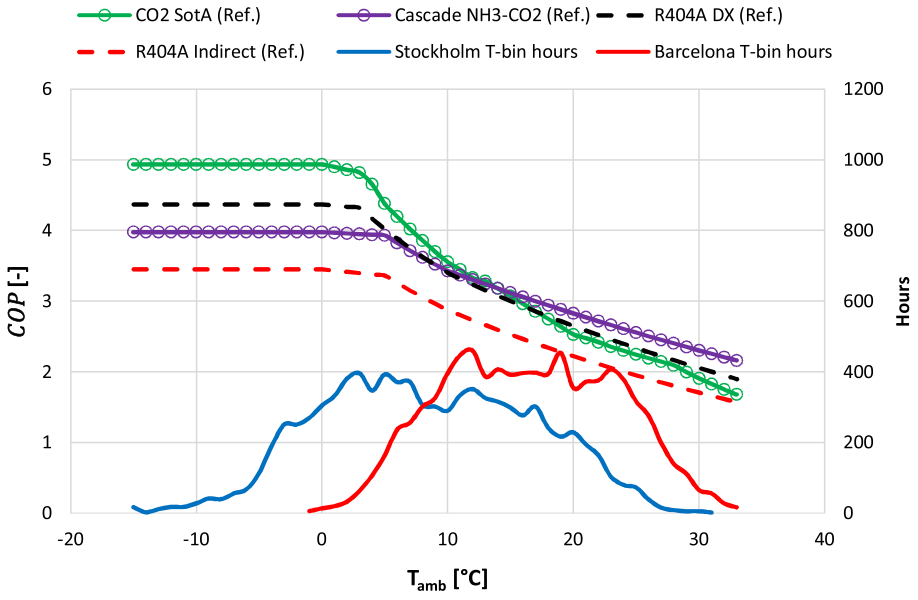

Fig. 14. Total refrigeration COP (COP_{ref}) – right and temperature-bin hours – left.

A common practice in some European countries is to have the condenser of this HFC/HFO indirect system in direct contact with the air (air cooled). If the condenser of the HFC/HFO indirect systems were assumed direct (air cooled), their energy efficiency could be increased by about 13%, compared to full indirect systems. This means these solutions would have rather comparable energy efficiency to full DX systems.

A key assumption for HFC/HFO DX systems is the minimum condensing temperature of 10 °C. This value is based on modern components and the smart control of floating condensing of an advanced HFC/HFO system. However, majority of these systems are run based on a more traditional value of 20–25 °C. If the minimum condensing temperature in HFC/HFO DX systems is assumed to be 20 °C, instead of 10 °C, the electricity saving would be reduced by 10% in Stockholm and by 2% in Barcelona, resulting in a saving of 1.2% in Stockholm and 14.1% in Barcelona for R404A DX and −3.3% and 11.3% in Stockholm and Barcelona respectively for R449A DX. −3.3% AEU savings means that R449A DX system consumes 3.3% more electricity than the standard CO_2 system annually in Stockholm. The reason that the Stockholm electricity savings is more affected by this assumption is that it runs for a longer period in the winter mode with minimum condensing temperature, in case of no heat recovery.

According to the results, the CO_2 state-of-the-art system is the most energy efficient solution in cold climates. Ammonia–CO_2 cascade solution has higher, R404A DX system has comparable, and R449A DX system has lower energy efficiency compared to the CO_2 state-of-the-art system in warm climates. However, these systems have some operation limitations.

Usage of ammonia or propane requires taking safety precautions. Compact designs and limiting the refrigerant charge will facilitate the application of this refrigeration solution. The relatively high GWP (about 1400 for R448A and R449A, and 1500 for R407H) and the amount of refrigerant charge in the HFC/HFO DX systems make this solution vulnerable to present and probable future environmental regulations. The high cost of these refrigerants and non-regulated price changes, similar to what is happening for R404A in its phase-out period, is another problem that these systems will face. Considering these environmental and economic restrictions, the HFC/HFO DX solution may not be considered a long-lasting solution, specifically for new installations.

The refrigeration COP of CO_2 SotA and three solutions presenting cascade, DX and indirect are shown in Fig. 14. As can be seen in the figure, COP_{ref} of CO_2 state-of-the-art system is higher than cascade NH_3–CO_2 and R404A DX system in ambient temperatures lower than about 13 and 18 °C, respectively. This crossover temperature for CO_2-R404A DX was about 21–26 °C according to other studies such as Finckh et al. (2011) if the minimum condensing temperature for HFC systems was assumed to be 20 °C. The COP of the HFC indirect system is the lowest compared to all the other three options. The crossover temperature for standard CO_2-R404A was about 23 °C in the authors' previous study (Sawalha et al., 2017) while this temperature for state-of-the-art CO_2 is about 33 °C, as shown in Fig. 14.

COP_{MT} and COP_{LT} are calculated to compare the systems' performance at two refrigeration temperature levels separately. In this way, the system is treated as two separate units for MT and LT, and can be compared to other system solutions. COP_{MT} and COP_{LT} values are presented in Fig. 15. These calculations are usually a challenge, since the amount of electricity use for interconnected LT and MT units are hard to break down. The method used to distinguish and separate electricity usage for LT and MT in the CO_2 systems and the definition of various COPs are discussed in detail in authors previous works, Karampour and Sawalha (2017) in Section 3.2 and Sawalha et al. (2015) in Section 3.5. The HFC system COPs are also studied closely by Sawalha et al. (2017) in Section 3.4. COP_{MT} and COP_{LT} for the cascade system are found based on a similar approach; the share of CO_2 MT loop and CO_2 LT loop loads on the total cooling load of high stage evaporator is calculated. The MT loop load consists of $\dot{Q}_{MT}$ and pump power and the LT load consists of $\dot{Q}_{LT}$ and LT compressor power $\dot{E}_{LT}$ [kW]. The amount of electricity use of high stage compressor and the indirect loop secondary fluid pump are divided between LT and MT loops based on their load shares.

4.2.2. TEWI comparison

The Total Equivalent Warming Impact (TEWI) is a greenhouse gas emissions (i.e. global warming impact) measure used to assess the direct and indirect global warming impacts of refrigeration systems. The direct impact originates from the refrigerant leakage and end-of-life disposal. The indirect impact is associated with the CO_2 emission content of the generated electricity, used by the refriger-

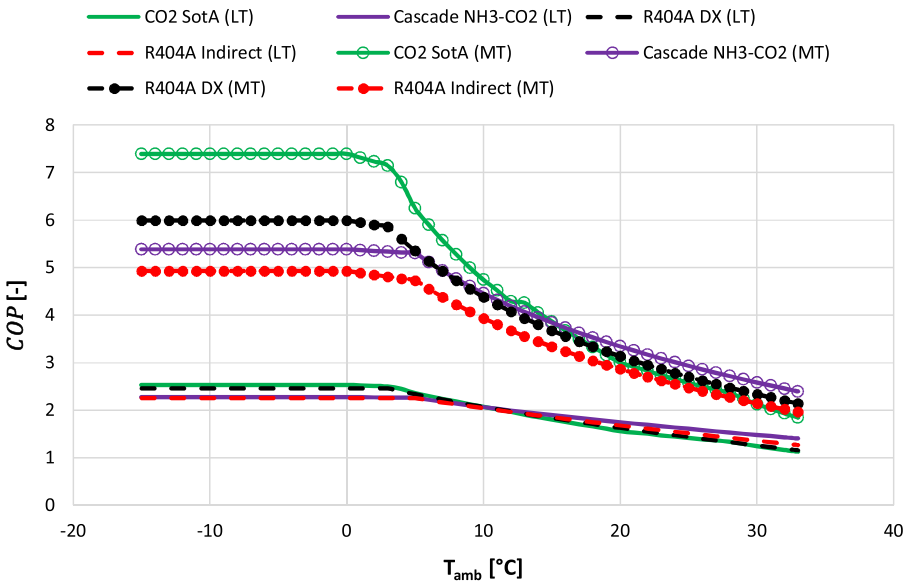

Fig. 15. Medium temperature COP (COP_{MT}) and low temperature COP (COP_{LT}).

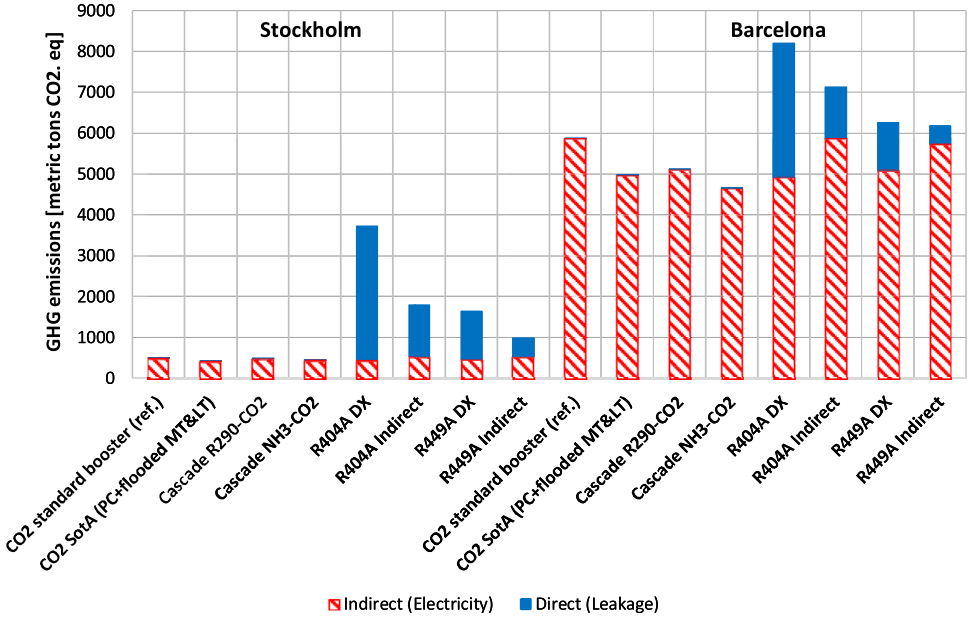

Fig. 16. TEWI comparison of refrigeration systems in Stockholm and Barcelona.

ation system. TEWI comparison provides a clear image of these impacts in the service lifetime of the refrigeration system. The TEWI of the eight systems are compared using the following correlation:

$$TEWI = \left(M_{leakage} \,.\, \mathrm{N} + \, M_{ref} .\, (1-\kappa)\right).\, GWP_{ref} + \mathrm{RC} \,.\, \mathrm{AEU} \,.\mathrm{N} \tag{11}$$

where $M_{leakage}$ is the refrigerant leakage per year [kg], N is the system lifetime, M_{ref} is the total refrigerant charge [kg], κ is the recycling factor, GWP_{ref} is the Global Warming Potential of the refrigerant and RC is the electricity regional conversion factor, CO_2 emission per unit of delivered electricity.

The first term in Eq. (10) represents the direct emissions due to refrigerant leakage, and the second represents the indirect emissions due to electricity use.

The assumptions made for this comparison are summarised in Table 3. In general, the indirect loops are assumed to contain less refrigerant charge and with lower leakage rates.

The results of the TEWI analysis are shown in Fig. 16. What can be observed is that the synthetic refrigerant-based refrigeration systems emit 2–7 times more greenhouse gases than the natural refrigerant-based refrigeration solutions during their lifetime in Stockholm. This enormous difference is clearly due to the leakage of high GWP synthetic refrigerants. Direct emissions are also high in Barcelona for the synthetic systems, however, it is not the major and only reason behind high GHG emissions of the systems.

The indirect emissions are significantly higher in Spain where 40–45% of the electricity is generated using fossil fuels (IEA, 2015), compared to 2–3% in Sweden (IEA, 2013). This makes the supermarket indirect emission impacts about 9 times higher comparing Spain to Sweden. This study shows that F-gas regulations can eliminate part of the negative environmental impacts of refrigera-

tion systems while the other part is connected to the production of low-carbon electricity.

This TEWI analysis compared different "refrigeration system" solutions. If heat recovery/heating and air conditioning are added to have "energy systems" TEWI analysis, the integrated CO_2 system would outperform the other cooling-heating alternatives more significantly in terms of being environmentally friendly.

5. Conclusion

This paper investigates the state-of-the-art modifications of a CO_2 trans-critical booster system so as to identify the most promising features in terms of energy efficiency. The impacts and limitations of these features are compared to the standard CO_2 system in Stockholm and Barcelona.

The results indicate that two-stage heat recovery, parallel compression, AC integration, and flooded evaporation are the important features of state-of-the-art integrated CO_2 systems. Some other modifications including mechanical sub-cooling and gas cooler evaporative cooling are considered as arbitrary options considering their impact and limitations.

According to the calculation results, heat recovery in two stages is an energy efficient solution to provide tap water heating and space heating demands. Space heating SPF_{HR} of the CO_2 system is about 10% higher than a stand-alone air source heat pump. Tap water heating is also provided by the CO_2 system with high average COP_{TWH} values of 5.4. The heating provided by CO_2 is about 50% cheaper than purchasing the heat from district heating network, and 20% cheaper than providing the heat by air source heat pump.

The air conditioning integration into CO_2 system is compared with a stand-alone AC system. $SEER_{AC}$ of the CO_2 system is comparable to stand-alone HFC-based AC system; about 4.5 in Stockholm and about 4 in Barcelona. Moreover, other factors including compactness and environmental considerations motivate the AC integration into CO_2 system. Parallel compression activation matches well with air conditioning.

Flooded evaporation and the methods to provide it are discussed. An evaporation temperature increase of 3–4 K in MT and LT levels results in energy saving of about 12% in Stockholm and Barcelona. Evaporation side modifications seem to be more consistent and promising compared to high pressure side modifications including mechanical sub-cooling and gas cooler evaporative cooling. Flooded evaporation is considered as a promising solution in warm and cold climates. The combined impact of using flooded evaporation at MT and LT levels, and parallel compression is about 13% in Stockholm and 17% in Barcelona.

The refrigeration performance of the state-of-the-art CO_2 system is compared to alternative refrigeration system solutions. These include cascade ammonia–CO_2 and propane–CO_2 solutions, and DX or indirect HFC/HFO solutions. Standard CO_2 refrigeration system is considered as the reference system. Comparison of annual energy use (AEU) in Stockholm shows that the state-of-the-art CO_2 system is the most energy efficient solution (15% AEU saving). Cascade ammonia–CO_2 and HFO/HFC DX systems are other energy efficient choices. The AEU comparison in Barcelona indicates that ammonia–CO_2 cascade has energy savings of about 20%, and the state-of-the-art CO_2 system and R404A DX follow these systems with about 15–16% AEU saving. R449A DX system is less efficient than the state-of-the-art CO_2 system both in warm and cold climates. This shows that the CO_2 system is even an efficient solution for warm climates.

The safety limitations of cascade solutions and the environmental-economic limitations of HFC/HFO systems might be some factors which make the state-of-the-art CO_2 system a favourable solution in both cold and warm climates. Furthermore, the integration of heating and AC makes this system a favourable all-in-one energy system. The cascade solutions can be considered as an alternative in warmer climates in case of satisfying the safety and risk issues. Using compact and low charge chillers facilitates this application. The synthetic refrigerant-based solutions have reasonable efficiency in warm climates, but are constantly subject to limitations of environmental regulations and long-term economic instabilities.

To conclude, the state-of-the-art integrated CO_2 system is energy efficient, environmentally friendly and compact solution able to provide the entire thermal demands of supermarkets efficiently in cold and warm climates.

Acknowledgement

The authors would like to acknowledge Swedish Energy Agency for funding this research through the Effsys Expand programme, Grant number 40338-1. The authors would also like to thank project industrial partners Advansor, Alfa Laval, Cupori, Energi & Kylanalys, Friginor, Green & Cool, Huurre, ICA, Industri & Laboratoriekyl and IWMAC.

References

Advansor, 2015. Will Bulgaria Make the Transition from CO2 Cascade to CO2 Transcritical?, retrieved 20.07.2017 from http://r744.com/articles/6313/will_bulgaria_make_the_transition_from_co_sub_2_sub_cascade_to_co_sub_2_sub_transcritical.

Arias, J., 2005. Energy Usage in Supermarkets-Modelling and Field Measurements (Doctoral Thesis). Royal Institute of Technology (KTH), Stockholm, Sweden.

Bertoldi, P., Cayuela, D.B., Monni, S., Piers de Raveschoot, R., 2010. Guidebook "How to Develop a Sustainable Energy Action Plan (SEAP)", EUR 24360 EN, available at: http://publications.jrc.ec.europa.eu/repository/bitstream/111111111/14204/1/com% 20 20 20g 20g g guidebook%20jrc%20format.pdf.

Beshr, M., Aute, V., Sharma, V., Abdelaziz, O., Fricke, B., Radermacher, R., 2015. A comparative study on the environmental impact of supermarket refrigeration systems using low GWP refrigerants. Int. J. Refrigeration 56, 154–164. doi:10.1016/j.ijrefrig.2015.03.025.

BITZER, 2017. Bitzer Semi-Hermetic Reciprocating Compressors, Selection Software, Retrieved 2017.04.15 from https://www.bitzer.de/websoftware/.

BITZER, 2016. Refrigerant Report 19, available at: https://www.bitzer.de/shared_media/documentation/a-501-19.pdf. Compact Mag. BITZER Kühlmaschinenbau GmbH.

Bush, J., Beshr, M., Aute, V., Radermacher, R., 2017. Experimental evaluation of transcritical CO_2 refrigeration with mechanical sub-cooling. Science and Technology for the Built Environment 23 (6), 1013–1025. doi:10.1080/23744731.2017.1289056.

Emerson Climate Technologies, 2010. Refrigerant Choices for Commercial Refrigeration Finding the Right Balance, available at: http://www.emersonclimate.com/europe/documents/resources/tge124_refrigerant_report_en_1009.pdf.

EU 517/2014, 2014. Regulation (EU) No 517/2014 of the European Parliament and of the Council, of 16 April 2014 on Fluorinated Greenhouse Gases, and Repealing Regulation (EC) No 842/2006.

Eurovent, 2017. Operational Manual for the Certification of Liquid Chilling Packages and Hydronic Heat Pumps.

Finckh, O., Schrey, R., Wozny, M., 2011. Energy and efficiency comparison between standardized HFC and CO_2 transcritical systems for supermarket applications. In: Presented at the 23rd IIR International Congress of Refrigeration, IIR/IIF. Prague, Czech Republic p. ID: 357.

Finckh, O., Sienel, T., 2010. Market introduction of commercially viable CO_2 supermarket refrigeration systems. In: Presented at the 9th Gustav Lorentzen Conference, IIR/IIF. Sydney, Australia.

Frigo-Consulting, 2014. Case study; Carrefour Alzira (ES), most southerly CO2 refrigeration system in Spain now in operation, Retrieved from http://www.frigoconsulting.ch/en/index.php?section=mediadir&cmd=casestudydetail&entryId=424.

Girotto, S., 2016. Direct space heating and cooling with CO_2 refrigerant. In: Presented at the ATMOsphere Europe 2016. Barcelona, Spain.

Girotto, S., Minetto, S., 2008. Refrigeration Systems for Warm Climates using only CO_2 as a Working Fluid. Natural Refrigerants. GIZ PROKLIMA https://www.giz.de/expertise/downloads/giz2008-en-natural-refrigerants.pdf.

Gullo, P., Cortella, G., 2016. Theoretical evaluation of supermarket refrigeration systems using R1234ze(E) as an alternative to high-global warming potential refrigerants. Sci. Technol. Built Environ. 22, 1145–1155. doi:10.1080/23744731.2016.1223996.

Gullo, P., Hafner, A., Cortella, G., 2017. Multi-ejector R744 booster refrigerating plant and air conditioning system integration – a theoretical evaluation of energy benefits for supermarket applications. Int. J. Refrigeration 75, 164–176. doi:10.1016/j.ijrefrig.2016.12.009.

Hafner, A., Banasiak, K., Herdlitschka, T., Fredslund, K., Girotto, S., Haida, M., Smolka, J., 2016. R744 ejector system, case: Italian supermarket, Spiazzo. In:

Presented at the 12th IIR Gustav Lorentzen Conference on Natural Refrigerants. Edinburgh, Scotland.
Hafner, A., Försterling, S., Banasiak, K., 2014. Multi-ejector concept for R-744 supermarket refrigeration. Int. J. Refrigeration 43, 1–13. doi:10.1016/j.ijrefrig.2013.10.015.
IEA, 2015. Energy Policies of IEA Countries: Spain, 2015 review, Available at http://www.iea.org/publications/freepublications/publication/IDR_Spain2015.pdf. International Energy Agency.
IEA, 2013. Energy Policies of IEA Countries: Sweden, 2013 review, http://www.iea.org/publications/freepublications/publication/Sweden2013_free.pdf. International Energy Agency.
IMST-ART, 2017. IMST-ART Advanced Refrigeration Technologies, retrieved 12.3.2017 from http://www.imst-art.com/.
IPU, 2017. IPU, Pack Calculation Pro, retrieved from: http://www.en.ipu.dk/Indhold/refrigeration-and-energy-technology/Pack%20Calculation%20Pro/Pack%20Calculation%20Pro.aspx. IPU.
Javerschek, O., 2008. Commercial refrigeration systems with CO_2 as refrigerant. In: Presented at the 8th IIR Gustav Lorentzen Conference on Natural Working Fluids. Copenhagen, Denmark.
Javerschek, O., Craig, J., Xiao, A., 2015. CO_2 as a refrigerant-straight right away!. In: Presented at the 24th IIR Refrigeration Congress of Refrigeration, IIR/IIF. Yokohama, Japan.
Javerschek, O., Reichle, M., Karbiner, J., 2016. Optimization of parallel compression systems. In: Presented at the 12th IIR Gustav Lorentzen Conference on Natural Refrigerants, IIR/IIF. Edinburgh, Scotland.
Karampour, M., Sawalha, S., 2017. Energy efficiency evaluation of integrated CO_2 trans-critical system in supermarkets: a field measurements and modelling analysis. Int. J. Refrigeration 82, 470–486. doi:10.1016/j.ijrefrig.2017.06.002.
Karampour, M., Sawalha, S., 2016a. Integration of heating and air conditioning into a CO_2 trans-critical booster system with parallel compression – part II: performance analysis based on field measurements. In: Proceedings of the 12th IIR Gustav Lorentzen Conference on Natural Refrigerants. IIR/IIF. Edinburgh, Scotland.
Karampour, M., Sawalha, S., 2016b. Integration of heating and air conditioning into a CO_2 trans-critical booster system with parallel compression – part I: evaluation of key operating parameters using field measurements. In: Proceedings of the 12th IIR Gustav Lorentzen Conference on Natural Refrigerants. IIR/IIF. Edinburgh, Scotland.
Karampour, M., Sawalha, S., 2015. Theoretical analysis of CO_2 trans-critical system with parallel compression for heat recovery and air conditioning in supermarkets. In: Proceedings of the 24th IIR Refrigeration Congress of Refrigeration. IIF/IIR. Yokohama, Japan.
Klein, S.A., 2015. Engineering Equation Solver (EES) V9, F-chart Software, Madison, USA, www.fchart.com.
Knudsen, H.-J.H., Pachai, A.C., 2004. Energy comparison between CO_2 cascade systems and state of the art R404A systems. In: Proceedings of 6th IIR-Gustav Lorentzen Natural Working Fluid Conference. Glasgow, UK.
Llopis, R., Nebot-Andrés, L., Cabello, R., Sánchez, D., Catalán-Gil, J., 2016a. Experimental evaluation of a CO_2 transcritical refrigeration plant with dedicated mechanical subcooling. Int. J. Refrigeration 69, 361–368. doi:10.1016/j.ijrefrig.2016.06.009.
Llopis, R., Sanz-Kock, C., Cabello, R., Sánchez, D., Nebot-Andrés, L., Catalán-Gil, J., 2016b. Effects caused by the internal heat exchanger at the low temperature cycle in a cascade refrigeration plant. Appl. Thermal Eng. 103, 1077–1086. doi:10.1016/j.applthermaleng.2016.04.075.
Lozza, G., Filippini, S., Zoggia, F., 2007. Using "Water-Spray" techniques for CO_2 gas coolers. In: Presented at the XII European Conference on "Technological Innovations in Air Conditioning and Refrigeration Industry,". Milan, Italy.
Makhnatch, P., Mota-Babiloni, A., Rogstam, J., Khodabandeh, R., 2017. Retrofit of lower GWP alternative R449A into an existing R404A indirect supermarket refrigeration system. Int. J. Refrigeration 76, 184–192. doi:10.1016/j.ijrefrig.2017.02.009.
Matthiesen, H.O., Madsen, K., Mikhailov, A., 2010. Evolution of CO_2 systems design based on practical experiences from supermarket installations in Northern Europe. In: Presented at the IIR Conference. Sydney, Australia.
Meteotest, 2016. Meteonorm Software V7. Bern, Switzerland, www.meteonorm.com.
Minetto, S., Brignoli, R., Zilio, C., Marinetti, S., 2014a. Experimental analysis of a new method for overfeeding multiple evaporators in refrigeration systems. Int. J. Refrigeration 38, 1–9. doi:10.1016/j.ijrefrig.2013.09.044.
Minetto, S., Girotto, S., Salvatore, M., Rossetti, A., Marinetti, S., 2014b. Recent installations of CO_2 supermarket refrigeration system for warm climates: data from the Field. In: Presented at the 3rd IIR International Conference on Sustainability and the Cold Chain, IIR/IIF. London, UK.
Nilsson, P.-O., Rogstam, J., Sawalha, S., Shahzad, 2007. Ice rink refrigeration system with carbon dioxide as secondary fluid in copper tubes. In: Proceedings of the 7th IIR Gustav Lorentzen Conference on Natural Working Fluids. Presented at the 7th IIR Gustav Lorentzen Conference on Natural Working Fluids. Trondheim, Norway.
Nöding, M., Fidorra, N., Gräber, M., Köhler, J., 2016. ECOS 2016: operation strategy for heat recovery of transcritical CO_2 refrigeration systems with heat storages. In: Presented at the 29th International Conference on Efficiency, Cost, Optimisation, Simulation and Environmental Impact of Energy Systems. Portorož, Slovenia.
Ommen, T., Elmegaard, B., 2012. Numerical model for thermoeconomic diagnosis in commercial transcritical/subcritical booster refrigeration systems. Energy Convers. Manag. 60, 161–169. doi:10.1016/j.enconman.2011.12.028.
Polzot, A., D'Agaro, P., Cortella, G., 2017. Energy analysis of a transcritical CO_2 supermarket refrigeration system with heat recovery. In: Proceedings of the 8th International Conference on Sustainability in Energy and Buildings, SEB-16, 11–13 September 2016. Turin, Italy, pp. 648–657. doi:10.1016/j.egypro.2017.03.227, 111.
Reinholdt, L., Madsen, C., 2010. Heat recovery on CO_2 systems in supermarkets. In: Proceedings of the 9th IIR Gustav Lorentzen Conference. Sydney, Australia.
Rogstam, J., 2016. CO_2 refrigeration systems evolution for ice rinks. ASHRAE J. 58 (10), 34–48.
Rogstam, J., Bolteau, S., 2016. Ice Rink of the Future, Evaluation of Energy and System Solutions, retrieved from http://www.ekanalys.se/assets/report-evaluation-of-gimo-ice-rink-15nov15-rev-04feb16.pdf.
Sawalha, S., 2013. Investigation of heat recovery in CO_2 trans-critical solution for supermarket refrigeration. Int. J. Refrigeration 36, 145–156.
Sawalha, S., 2008. Carbon Dioxide in Supermarket Refrigeration (Doctoral Thesis). Royal institute of technology (KTH), Stockholm, Sweden.
Sawalha, S., Karampour, M., Rogstam, J., 2015. Field measurements of supermarket refrigeration systems. Part I: analysis of CO_2 trans-critical refrigeration systems. Appl. Thermal Eng. 87, 633–647. doi:10.1016/j.applthermaleng.2015.05.052.
Sawalha, S., Perales, C.C., Likitthammanit, M., Rogstam, J., Nilsson, P.-O., 2007. Experimental investigation of NH_3/CO_2 cascade system and comparison to R404a system for supermarket refrigeration. In: Proceedings of the 22nd International Congress of Refrigeration. Beijing, China.
Sawalha, S., Piscopiello, S., Karampour, M., Manickam, L., Rogstam, J., 2017. Field measurements of supermarket refrigeration systems. Part II: analysis of HFC refrigeration systems and comparison to CO_2 trans-critical. Appl. Thermal Eng. 111, 170–182. doi:10.1016/j.applthermaleng.2016.09.073.
Schönenberger, J., Hafner, A., Banasiak, K., Girotto, S., 2014. Experience with ejectors implemented in a R744 booster system operating in a supermarket. In: Presented at the 11th IIR Gustav Lorentzen Conference on Natural refrigerants, IIR/IIF. Hangzhou, China.
Shecco, 2016. Guide 2016: Guide to Natural Refrigerants in Japan – State of the Industry, retrieved from: http://publication.shecco.com/publications/view/65. Brussels, Belgium.
Shecco, 2015. Guide 2015: Guide to Natural Refrigerants in North America-State of the Industry, retrieved from: http://www.publications.shecco.com/publications/view/guide-north-america-2015. Brussels, Belgium.
Simard, L., 2012. Ice rink uses CO_2 system. ASHRAE J. 54 (3), 38–44.
Tambovtsev, A., Quack, H., 2007. COP improvement by transfer of the superheating into the internal heat exchanger. In: Presented at the International Congress of Refrigeration. Beijing, China.
Tsamos, K.M., Ge, Y.T., Santosa, Id., Tassou, S.A., Bianchi, G., Mylona, Z., 2017. Energy analysis of alternative CO_2 refrigeration system configurations for retail food applications in moderate and warm climates. Energy Convers. Manag. doi:10.1016/j.enconman.2017.03.020.
Zeiger, B., Gschrey, B., Kauffeld, M., 2016. Availability of Alternatives to HFCs in Commercial Refrigeration in the EU, retrieved from: https://ec.europa.eu/clima/sites/clima/files/20161201_briefing_supermarket_en.pdf.